Available online at www.sciencedirect.com

ScienceDirect

Geochimica et Cosmochimica Acta 288 (2020) 262–281

Geochimica et Cosmochimica Acta

www.elsevier.com/locate/gca

Geochemical transformations beneath man-made ponds: Implications for arsenic mobilization in South Asian aquifers

Mason O. Stahl [a,*], A.B.M. Badruzzaman [c], Mehedi Hasan Tarek [c], Charles F. Harvey [b]

[a] Department of Geology, Union College, Schenectady, NY, USA
[b] Department of Civil and Environmental Engineering, Massachusetts Institute of Technology, Cambridge, MA, USA
[c] Department of Civil and Environmental Engineering, Bangladesh University of Engineering and Technology, Dhaka, Bangladesh

Received 4 September 2019; accepted in revised form 11 August 2020; available online 20 August 2020

Abstract

The role of man-made ponds on arsenic mobilization was examined in Bangladesh. Here, we describe a field experiment that shows how recharge from a newly constructed pond creates a reactive front that moves downward into the underlying aquifer, but only advances slowly, less than 8 cm/year. We found that pond recharge introduces organic carbon that likely drives the reduction of sulfate and solid-phase iron. However, over the six-year period of the study the pond did not drive arsenic contamination of the underlying groundwater. An electron balance indicates that significant precipitation of ferrous iron and sulfide minerals may immobilize arsenic despite the shift towards more reducing conditions, explaining the very low observed aqueous arsenic concentrations. We additionally found that the amount of solid-phase electron acceptors available in the shallow sediments strongly retards the advance of a reduced sediment front. Our results suggest that labile organic carbon introduced by man-made ponds is efficiently mineralized in the sediments immediately below the pond bottom and thus is unlikely to drive arsenic mobilization deeper within the aquifer. We suggest that the excavation of man-made ponds removes young surficial sediments, leaving aged and less reactive sediments beneath the pond, so that recharge through excavated ponds does not mobilize arsenic at the high rates observed in recharge through natural wetlands and river banks.

Keywords: Arsenic; Iron; Organic carbon; Ponds; Redox; Groundwater quality; Groundwater recharge; Bangladesh

1. INTRODUCTION: PONDS, AQUIFER RECHARGE, AND GROUNDWATER ARSENIC

Contamination of groundwater with geogenic arsenic (As) is widespread throughout Bangladesh and much of South and Southeast Asia damaging the health of millions of people who consume this water (Smith et al., 2000; Argos et al., 2010). This issue came to light in the mid 1990's and since then geochemical studies have reached a general consensus that the dominant mechanism of As mobilization is microbially-mediated oxidation of organic carbon (OC) coupled to the reductive dissolution of As-bearing iron-oxide minerals contained within the aquifer sediments (Nickson et al., 2000; McArthur et al., 2001; Harvey et al., 2002; Swartz et al., 2004; Horneman et al., 2004; Postma et al., 2007, 2010). The cause of spatial variability in As concentration, both laterally and with depth, found in aquifers throughout South and Southeast Asia remains incompletely understood.

* Corresponding author.
E-mail address: stahlm@union.edu (M.O. Stahl).

https://doi.org/10.1016/j.gca.2020.08.012
0016-7037/

Concentrations of dissolved As vary from below WHO guidelines (10 μg/L) to levels one or two orders of magnitude above these guidelines over the sub-kilometer scale between wells at a given depth and over the vertical scale of meters at a given location (BGS and DPHE, 2001; Yu et al., 2003). Recharge conditions and flow patterns may in part explain some of the observed patterns in groundwater As (Weinman et al., 2008). However, it is unclear whether high levels of groundwater As develop as a result of recharge from specific sources such as ponds, wetlands, rivers and, if so, how these recharge sources have affected the overall distribution of groundwater As contamination (Polizzotto et al., 2008; Sengupta et al., 2008; Neumann et al., 2010; Datta et al., 2011; McArthur et al., 2011; Lawson et al., 2013; Stahl et al., 2016; Nghiem et al., 2019). Resolving these questions is important for identifying how the current levels of dissolved As reached their present state and for making predictions about how aquifer systems will respond to perturbations that affect recharge such as changes in land use, intensive groundwater pumping, and changing climate.

Redox gradients are generally steep in the near-surface environment and thus these zones are often sites of more active redox cycles relative to deeper sediments. In particular, surface sources may introduce reactive OC to the aquifer, which could stimulate As mobilization along a recharge flow-path. Recharge passing through ponds and wetlands with perennially saturated sediments will not have passed through an oxic unsaturated zone and therefore may reach the aquifer with anoxic conditions that favor As mobilization. The reactivity of sediment organic matter and iron-oxides as well as the solid-phase ratio of As:Fe has been observed to decrease with sediment age for Holocene aquifers in South and Southeast Asia (Dowling et al., 2003; Postma et al., 2010, 2012) suggesting that the shallow sediments beneath surface bodies of water may be relatively reactive. Furthermore, solid-phase As concentrations in shallow sediments are generally greater than those of deeper aquifer sediments and are at levels sufficient to sustain high concentrations of dissolved As (i.e. >100 ppb) for many pore volumes of flushing (Harvey et al., 2002; Swartz et al., 2004). Thus, conditions directly beneath ponds and wetlands may be conducive to the near-surface mobilization of significant quantities of As, which could then be advected deeper into the aquifer (Polizzotto et al., 2008; Stuckey et al., 2016). This could potentially result in high groundwater As concentrations even if no additional As mobilization were to occur within the aquifer.

Even without variations in recharge chemistry, spatial variations in recharge quantity across the land surface may also affect groundwater As concentrations. Dissolved As may accumulate in stagnant areas with little recharge and concentrations will be diluted where large recharge fluxes flush the aquifer (Jakobsen et al., 2018). In this case, enhanced recharge from ponds would lower As concentrations simply by dilution. Considering the potential for both enhanced geochemical mobilization and enhanced flushing, it seems likely that pond recharge plays some role in the pattern of groundwater arsenic concentration.

In the Bengal Basin, man-made ponds are ubiquitous, with more than 4 million households owning a pond and cover an estimated 2.6% of the area of Bangladesh (Belton and Azad, 2012). These ponds are a significant source of recharge (Harvey et al., 2006; Stahl et al., 2014) and they have been implicated as an important source of organic carbon for fueling As mobilization (Neumann et al., 2010), which suggest they may play a critical role in the groundwater As contamination observed throughout that region. However, the widespread presence in villages of man-made ponds represents a relatively recent perturbation to these aquifer systems as most ponds were constructed in the past 70 years (Kränzlin, 2000). Thus, characterizing the source and age of the organic matter driving redox processes within these aquifers is central to assessing the role of man-made ponds on As contamination and has been an area of significant research and debate. Harvey et al. (2002) argued that the young radiocarbon ages of DIC and methane found at the depths where peak arsenic concentrations occur suggest that young, surface derived OC is likely driving As mobilization. Consistent with the work of Harvey et al. (2002), Neumann et al. (2010) presented results suggesting that irrigation pumping focuses pond recharge at the depth where the highest levels of groundwater As are observed and that reactive OC sourced from man-made ponds is a key driver of As mobilization. Working in West Bengal and Cambodia, Lawson et al. (2013 and 2016) present radiocarbon dates of groundwater DOC which indicate that modern surface derived OC is transported to depths >30 m, a result that suggests recent anthropogenic perturbations such as pond construction could potentially be responsible for the presently observed patterns of dissolved As. Mailloux et al. (2013) concluded that advected OC controls the redox status of an As affected aquifer in Bangladesh, however they argued advected OC is retarded relative to groundwater flow thus precluding the recent (<100 yrs) anthropogenic perturbations of man-made ponds and irrigation pumping from manifesting at depth. Further complicating the issue are the numerous studies that argue against the role of surface-derived OC in controlling As mobilization – suggesting instead that sedimentary organic matter is the primary redox driver in As affected aquifers across South and Southeast Asia (McArthur et al., 2004; Postma et al., 2007; Mladenov et al., 2010; Datta et al., 2011; Desbarats et al., 2014). Thus, at present the role of man-made ponds as a driver of groundwater As contamination in the Bengal Basin remains unclear.

While it is understood that constructed ponds have significantly changed the quantities and patterns of recharge in Bangladesh (Harvey et al., 2002, 2006; Neumann et al., 2010), no prior studies have directly looked at and tracked through time As mobilization beneath constructed ponds. Here we present results from an experimental pond that was studied over a six year period to test the hypothesis that pond recharge is a driver of groundwater As contamination in Bangladesh (Harvey et al., 2002; Neumann et al., 2010). In addition to examining if man-made ponds cause groundwater As contamination, we also ask the questions: How does a newly excavated pond affect underlying groundwater

chemistry? How does the solute load carried by recharge from the pond chemically interact with the underlying sediment? What controls the rate of migration of the reactive front?

To address these questions, we measured geochemical conditions before and after construction of a pond, tracing the geochemistry in the sediments and aquifer underlying the pond for over six years after construction of the pond. We describe results from analysis of the geochemistry of the pond water, shallow groundwater and sediment beneath the pond. We present a detailed electron balance to identify the likely redox processes occurring as pond water recharges the shallow sediments. For the first time, we provide direct observations and quantification of the geochemical processes that occur as recharge flows from man-made ponds and into the underlying aquifer. We use these findings to generate a prediction of how As concentrations and redox conditions beneath our study pond may evolve over time and to better describe the role of ponds in As mobilization in Bangladesh. Finally, we contextualize our findings within the broader context of the role of surface water recharge on As mobilization and present a conceptual model that identifies how the unique features of man-made ponds relative to naturally occurring surface water bodies influences their ability to drive As contamination.

2. FIELD SITE

We partnered with a local farmer to construct a pond on land used for rice cultivation. Before the pond was constructed, we installed a network of pore water samplers, wells, and water level loggers beneath and around the pond area. Then we tracked the hydrologic and geochemical transformations beneath the pond that occurred as the result of the pond over the course of several years.

The field site is located in Munshiganj, Bangladesh approximately 20 km south of Dhaka, 10 km north of the Ganges (Padma) River, and 25 km west of the Meghna River (Fig. 1). Within the village of Bashailbhog which surrounds our field site, irrigated rice fields cover approximately 65% of the land area while ponds and village areas cover 11% and 22% of the land area respectively (Harvey et al., 2006; Neumann et al., 2010). Rice fields are irrigated by wells spaced 100′s of meters apart that are mostly screened at 30 to 40 m depth. As a result of irrigation pumping, groundwater generally flows laterally towards irrigation wells with a downward component in the upper 30–40 m of the aquifer (Harvey et al., 2006; Neumann et al., 2010). The field area is annually inundated under 3–4 m of water during the monsoon season, with the floods generally coming in July and receding around November, leaving the ponds full at the start of the dry season. During monsoon flooding much of the landscape is covered by aquatic plants (Supplementary Fig. 7), however landowners generally remove these plants from ponds prior to the end of the monsoon floods (Supplementary Fig. 8).

The geochemistry and hydrology of this site have been the subjects for a set of previous papers. Solid and dissolved aquifer chemistry were described for a site 1 km northwest in Harvey et al. (2002), Swartz et al. (2004), Polizzotto et al. (2006) and in Hug et al. (2011). The hydrology was described in Harvey et al. (2006), Klump et al. (2006),

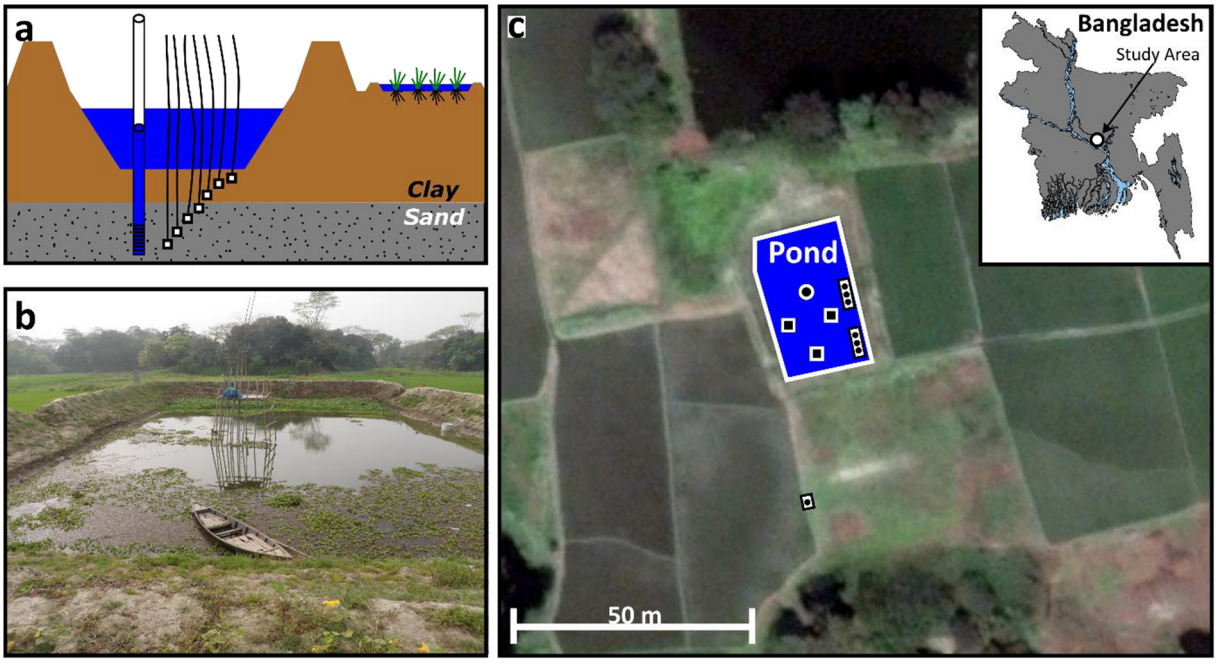

Fig. 1. (a) Illustration of the study pond and shallow samplers beneath the pond. Shallow well located in the center of the pond is shown and the white squares represent the lysimeter and drive-point samplers. (b) Photo of the study pond. (c) Satellite image of the field site with the study pond shown as a blue polygon outlined in white. Symbols indicate sampling points (circles represent wells, circles in bounding box represent of drive-point wells, each square represents a cluster of four lysimeters). Note the drive-point well adjacent to a rice field, approximately 30 m south of the study pond. Inset map shows the location of the study site.

and Neumann et al. (2010). Rice field hydrology and geochemistry has been described in Neumann et al. (2009, 2010, 2011), Polizzotto et al. (2013), Roberts et al. (2007, 2011), and Dittmar et al. (2007).

2.1. Pond construction

Our observations during pond excavation and well/lysimeter installation reveal that the shallow aquifer at our field site is composed of alternating beds of silts and sands and is overlain by a three-meter thick clay layer that extends to the land surface. The pond was constructed following local practice, with a team of ~40 workers manually excavating a 25 m × 30 m pit from the upper two meters of the three meter thick surficial clay and building a 1.5 m high berm around the pond (see photos in supplementary material) so that the pond has a depth of about 3.5 m when at the highest water level and is underlain by 1.0 ± 0.2 m of clay remaining of the 3 m layer. Prior to the installation of the pond the land had been used as a rice field. The raised barrier around the pond is annually overtopped by monsoon floodwaters and the water level in the pond remains higher than the elevation of the water table after the floods recede, producing a downward gradient that drives aquifer recharge (see Stahl et al., 2014 and supplementary material). The study pond contains water throughout the year and while the water level falls during the dry season it does not at any point go dry.

2.2. Recharge fluxes from the pond and crab burrows

In an earlier paper (Stahl et al., 2014), we characterized the hydrology of the pond. We combined hydraulic measurements with measurements of shifts in stable water isotopes due to evaporation to quantify the recharge delivered by the pond to the aquifer. We estimated an annual average flux of 223 cm/yr (specific discharge), a flux that is 2.2 times larger than the estimated flux of 103 cm/yr from surrounding rice fields (Neumann et al., 2009). While the pond is discharging to the underlying aquifer through its bottom sediments, from around January through March water is also flowing into the pond through the sides from neighboring irrigated rice fields (Stahl et al., 2014). Thus, the total recharge from the pond is greater than the difference between the decrease in pond volume and the loss to evaporation.

Terrestrial crabs, which are widely found throughout Bangladesh (Rahman et al., 2008), create burrows at our site which perforate the clay layer separating the pond from the underlying sand and silt aquifer (Stahl et al., 2014). The preferential flow paths created by crab burrows in the clay underlying local ponds increase the hydraulic conductivity by a factor of 100 as compared to the undisturbed clay (i.e., from $4 * 10^{-4}$ to $4 * 10^{-2}$ m/day), thus channeling most of the recharge through crab burrows (Stahl et al., 2014). Thus, these burrows, which exist through the surficial clay layer, act to greatly enhance recharge through the surficial clays across both pond and non-pond covered areas throughout the region. These burrow act as preferential flow paths that allow much of the recharging water to bypass the clay and flow into the underlying sand/silt (Figs. 2 and 3) where the non-cohesive nature of the sand/silt does not support the presence of crab burrows (Wagle, 1924; Stahl et al., 2014).

3. METHODS

3.1. Well, drive-point, and lysimeter installation

To monitor the chemical and hydrologic conditions directly beneath the pond we installed a cluster of 8 monitoring wells in the center of the pond (6.1 m, 7.6 m, 9.1 m, 12.2 m, 15.2 m, 19.8 m, 24.4 m, and 30.5 m below land surface) with the bottom 1 m of the well screened to the aquifer (Fig. 1). We also installed three clusters of lysimeters and two clusters of shallow drive-point wells to allow for the geochemical characterization of shallow groundwater beneath the pond. Each lysimeter cluster contained four lysimeters (0.25 m, 0.5 m, 1.0 m, and 1.5 m below the pond bottom) and each drive-point cluster contained 3 drive-point wells (2.0 m, 2.8 m, and 3.5 m below the pond bottom) (see Fig. 1). We also installed a drive-point (3.8 m below land surface) approximately 30 m from our pond and adjacent to a rice field. Thus, there is a total of 8 monitoring wells, 12 lysimeters and 7 drive-point wells, for a total of 27 sampling locations.

Monitoring wells were installed using the local "hand-flapper" installation method (see supplementary material for in-depth description). The monitoring wells were cased with 5.1 cm (2 inch) ID PVC pipe. The bottom 1 m of the pipe consists of slotted PVC, which allows exchange between the aquifer and the well.

Stainless steel drive-points (Solinst Model 615) were installed in the shallow aquifer beneath the pond (<6.1 m below land surface) to allow for the collection of shallow groundwater samples. The drive-points were installed by drilling a hole using a modified version of the technique as described for well installation (see supplementary material for additional details).

Lysimeters (Prenart Super Quartz) were installed in the shallow (<2 m) sediments beneath the pond to allow for the collection of porewater samples. The lysimeters were installed by pushing the lysimeter into an augered hole and backfilling the hole with the augered sediments. The lysimeters were purged following installation and then allowed to equilibrate for several months prior to the collection of water samples.

The lysimeters at 0.25 m, 0.5 m, 1.0 m below the pond bottom all lie within the clay layer that extends to 1 m below the base of the pond. Our deepest lysimeters (1.5 m below the pond) are approximately 50 cm into the sand/silt layer – thus these samplers collect recharging pond water after it has likely moved down a crab burrow, bypassing the 1 m thick clay layer, and then flowed ~50 cm into the sand/silt matrix (Fig. 3).

3.2. Field sampling and analysis of water

Samples from monitoring wells were collected after lowering the pump to the depth of the well screen purging for at least five minutes. Electrode measurements (pH, DO,

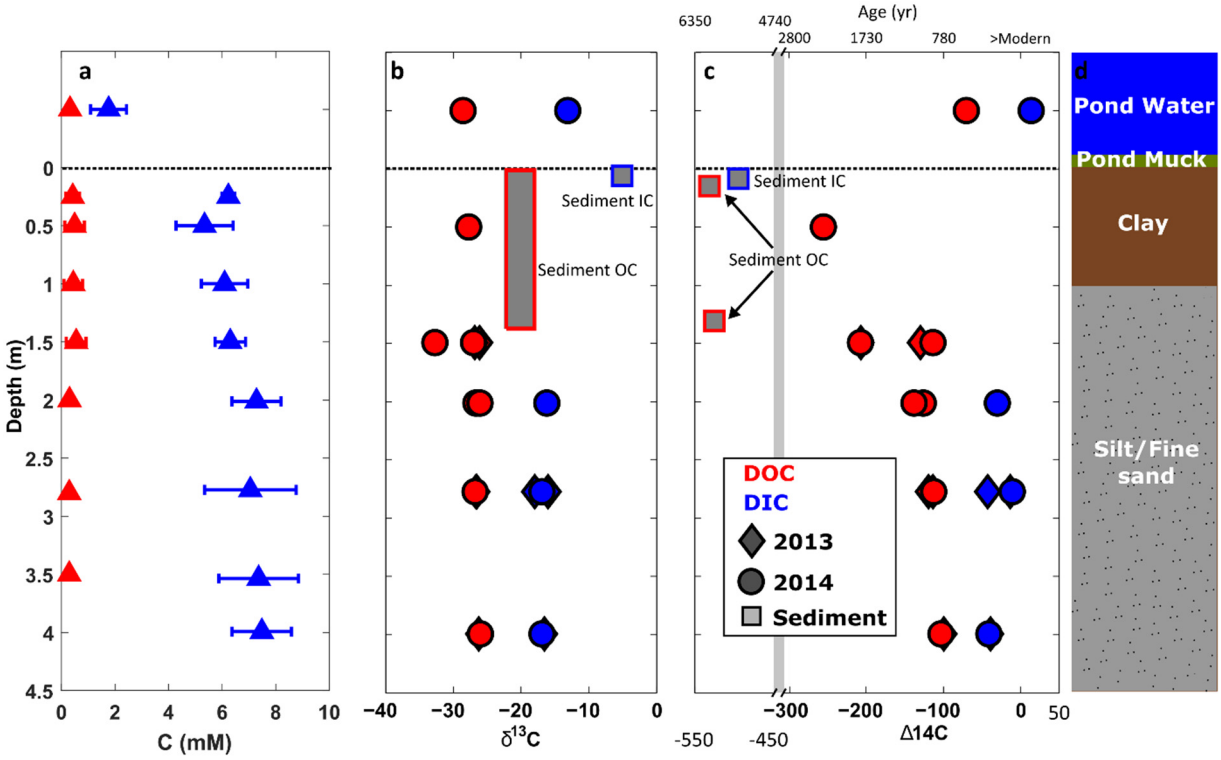

Fig. 2. Depth profiles of aqueous and solid-phase carbon beneath the study pond (all depths relative to pond bottom). The dashed line represents the pond bottom. Pond water samples are shown above the dashed line representing the pond bottom. (a), Average DOC (red triangles) and DIC (blue triangles) concentrations with horizontal bars representing the standard deviations. (b), $\delta^{13}C$ of DOC, DIC, sediment OC, and sediment IC. Sediment OC $\delta^{13}C$ represents the range measured on 11 samples collected 9 months post pond construction from upper 1.3 m. (c), $\Delta^{14}C$ of DOC, DIC, sediment OC, and sediment IC (^{14}C ages shown on top axis). In panels b and c samples collected in 2013 and 2014 are represented by diamonds and circles respectively. (d), diagram of pond water column and sediments. (For interpretation of the references to colour in this figure legend, the reader is referred to the web version of this article.)

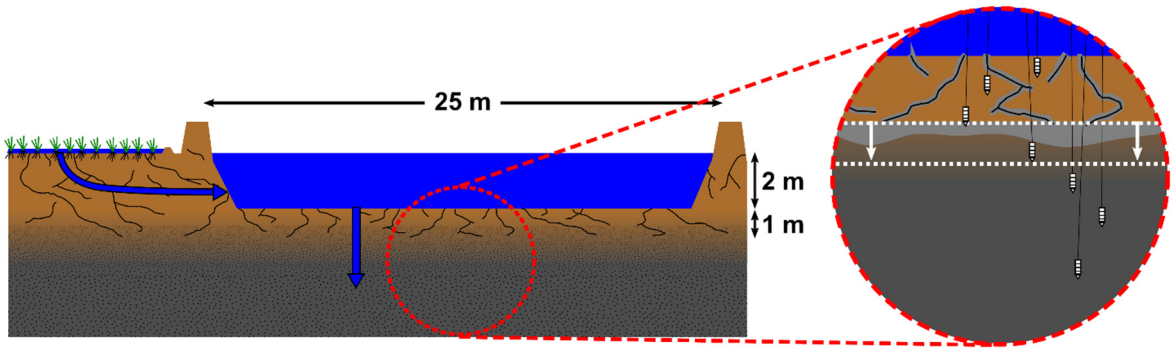

Fig. 3. Schematic illustrating the influence of crab burrows on recharge pathways beneath a man-made pond. The black lines represent the burrows and the gray area around the burrows represents the area of reduced sediment that is likely generated around the burrows as recharging pond water flows out of the burrow and into the sediment matrix. The white dashed lines represent the start and end of the flow-path described in Section 5.1.2. Given the dense network of crab burrows, the shallow samplers beneath the pond all collect water that has flowed roughly the same distance through the sediment matrix (i.e. distance from burrow or pond bottom to sampling point). Thus, the chemistry data will be similar for these sampling points and a typical vertical chemical depth profile is not observed.

EC, temperature) were taken by pumping the water into a flow-through-cell containing electrodes and were recorded once the readings had stabilized. Water was sampled downstream of a filter (0.45 um Versapor filter for ICP-MS/OES analysis and 0.2 um PES filter for DOC analysis), following the protocol outlined in Supplementary Table 1 immediately after electrode readings were taken. Surface water samples were collected by lowering a pump approximately 0.3 m beneath the water surface and pumping the water into a flow-through-cell containing electrodes described

above. Once the electrode readings were taken, samples were collected as outlined in Supplementary Table 1.

Groundwater samples were collected from the smaller-diameter drive-points using a peristaltic pump. Drive-points were purged prior to sample collection. Electrode measurements and water samples were collected in the same manner as described for monitoring wells.

Prior to sampling, lysimeters were purged for at least 6 hours. Lysimeter samples were collected by attaching a 1 L volume polypropylene-lined foil bag (SKC Flex Foil bags) to the lysimeter tubing. The bag was first purged with argon or nitrogen gas prior to attaching to the lysimeter tubing. The purged bag was then placed into a glass vacuum chamber and a vacuum was pulled, causing water to flow into the sample bag. Water flow from lysimeters was generally slow so sample collection usually commenced in the evening and the sample was collected the following morning. Once the full sample bag was collected electrode measurements and water samples were collected. A syringe was attached to the nozzle of the sample bag and water was drawn into the syringe. This was then carefully dispensed into a small cup containing the pH, EC and temperature electrodes and readings were taken. Water was again drawn from the bag and into a syringe and this water was dispensed into sampling bottles using syringe filter versions of the filters described in Supplementary Table 1.

3.3. Laboratory analysis of water

Measurements of Na, Mg, Si, P, S, K, Ca, Mn, Fe, and Sr were done by ICP-OES (Perkin Elmer Optima 7300 DV). Linear calibration curves for each element were generated using multi-element standards run at the beginning of the analysis. A subset of the standards was run every 10–12 samples along with certified reference waters (Environment Canada waters TMDA-64.2 and MISSIPPI-03). An internal standard solution of Yttrium was run with every sample to correct for instrument drift.

Measurements of As were done by ICP-MS (Perkin Elmer Elan DRC-II or Agilent 8900). The instrument was operated in dynamic reaction mode with an oxygen reaction cell in order to prevent interference from ArCl that can occur when chloride from the sample reacts with the argon gas used to generate the plasma.

Chloride and Br were measured by ion chromatograph (Dionex ICS3000) and DOC was measured by TOC analyzer (Shimadzu TOC-VCPH) after the samples were acidified (with HCl) and sparged with nitrogen gas to remove DIC.

Stable water isotopes of hydrogen and oxygen were measured by isotope ratio infrared spectroscopy (IRIS) on a wavelength-scanned cavity ring-down spectrometer (WS-CRDS) (Picarro L1102-i). Samples were analyzed against lab reference materials that have been calibrated to Vienna Standard Mean Ocean Water (VSMOW).

Alkalinity was measured by Gran Titration within 48 hours of sample collection. Titrations were done using 0.02 N sulfuric acid delivered by burette. The sample was stirred continuously during the titration using a magnetic stir bar on a stir plate. Ammonium was measured spectrophotometrically (Hach DR2500) using the Nessler method.

Measurements of $\Delta^{14}C$ were done by accelerator mass spectrometry (AMS) on carbon that had been extracted from the sample and converted to graphite. DOC samples are oxidized to CO_2 by UV oxidation and the CO_2 is sparged from the water sample and converted to graphite (see Beaupré et al., 2007 for details). DIC samples are acidified and sparged and the evolved CO_2 is converted to graphite. Measurements of $\delta^{13}C$ were done by stable isotope mass spectrometer and these values were used to correct the $\Delta^{14}C$ values for fractionation effects. These measurements and all sample preparation were performed at the Woods Hole Oceanographic Institute NOSAMS lab.

3.4. Sediment sampling and analysis

Samples were collected by hammering a stainless steel core sampler with a 5.1 cm ID × 30.5 cm L PVC core tube liner into the sediments. The corer was then pulled out and additional cores could be collected in 30.5 cm intervals following the procedure above. Once the corer was pulled out, the core tube containing the sediment was removed and sealed with plastic caps on each end. The caps were secured with electrical tape and the core was placed into an oxygen barrier bag (ESCAL film) and oxygen scavenging packets were placed into the bag. The bag was promptly sealed using a heat sealer and the packaged core was stored under refrigeration.

Prior to analysis, sediments were extruded from the core tubes, divided into segments of approximately 7 cm in length and dried in a drying oven at 50 degrees Celsius for 48 hours. The dried segments were then ground by mortar and pestle to homogenize each sample segment before analysis.

Total carbon was measured on a CNHS elemental analyzer (Carlo Erba NA1500). Inorganic carbon was measured coulometrically using a UIC CO_2 coulometer (Coulometrics 5011). Measurements of $\delta^{13}C$ of sediment organic matter were done on samples that were acidified to first remove the IC. The $\delta^{13}C$ of organic matter was measured by combusting the sample and introducing the evolved CO_2 to an isotope ratio mass spectrometer (Thermo Electron DeltaV Advantage). Inorganic $\delta^{13}C$ was also measured by isotope ratio mass spectrometry by acidifying the sample and measuring the isotopes of the evolved CO_2. Measurement of $\Delta^{14}C$ for sediment organic and IC was done methods similar to those described in Section 3.3.

Total elemental composition of sediment samples were measured by X-ray fluorescence spectroscopy (XRF) on a Bruker S8 Tiger XRF. Prior to analysis samples were dried and ground using a mortar and pestle. Quantitative mineralogical analysis of sediments was done by X-ray diffraction (XRD). The samples were analyzed on a diffractometer using a Cu tube (Bruker D4 Endeavor). The intensity data was converted to concentrations using whole pattern fitting with empirically-derived internally consistent relative intensity ratios and reference spectra from the American Mineralogist Crystal Structure Database (Downs and

Hall-Wallace, 2003). The samples were glycolated prior to analysis to allow for the identification of swelling clays.

Measurements of the magnetic fraction of the sediments were done using a hand magnet to separate out the magnetic portion of a sample. Prior to magnetic separation, sediment samples were ground and homogenized using a mortar and pestle. The sample was weighed using a digital balance and then a hand magnet was repeatedly passed over the sample to collect the magnetic fraction. The collected magnetic fraction was then weighed to allow for the determination of the fraction of the total sample that was magnetic.

3.5. Speciation modeling

Calculations of mineral saturation indices were performed using the PHREEQC geochemical modeling software (USGS) with the PHREEQC thermodynamic database. Calculations of mineral saturation indices at each aquifer depth were done using the mean values for aqueous chemical parameters measured at that depth as the model inputs. Mineral stability diagram were produced in Geochemist's Workbench using the LLNL thermodynamic database (Johnson et al., 2000).

4. RESULTS

4.1. Aqueous geochemistry: Within and below the pond

Water chemistry data collected on our study pond and the lysimeters, drive-points, and shallow wells beneath our pond are summarized in Table 1 (see supplementary data file for all the underlying data). The shallow groundwater below the pond is a calcium-bicarbonate type water with subordinate amounts of sodium and magnesium, near neutral pH ranging from 6.7 to 7.3, and is near saturation with respect to calcite and super-saturated with respect to siderite and rhodochrosite (Table 2). Specific conductance increases from the pond to the underlying aquifer, with an average value of 217 μS/cm in the pond and 563 μS/cm in the porewater at 1.5 m beneath the pond bottom (3.6 m below land surface). We also collected shallow groundwater from an area adjacent to a rice field and we find similar chemistry to that of the shallow groundwater recharged by the pond (Table 1).

Mean As concentrations are very low (<0.1 μM) in the surface water and shallow groundwater below the pond. Dissolved inorganic (DIC) increases dramatically (>4 mM increase from 2.03 mM to 6.09 mM at 1 m depth) as pond water flows into the shallow sediments (<5 m BLS), indicative of the oxidation of organic matter (solid-phase carbonates are in very low abundance). Dissolved organic carbon (DOC) concentrations increase from a mean of 0.33 mM in the pond water to a mean value of 0.55 mM in the shallow groundwater at 1.5 m beneath the pond (3.6 m BLS) (Fig. 2 and Table 1). The increase in DOC from pond water to the shallow sediment, suggests that OC from a solid-phase source is leaching into the recharging water.

Data collected over the course of the study for the shallow groundwater beneath the pond (lysimeter samples from 0.25 to 1.5 m below the pond bottom) provide an indication of how concentrations have responded following construction of the pond (Fig. 4). Linear regression fits computed on the time series concentration data for each lysimeter sampling location allow for an assessment of temporal trends. The majority of the lysimeters exhibit decreasing trends with time (negative slope with p-value < 0.05) for Na, Si, Ca, Mg, Mn, and Sr, with none of the lysimeters exhibiting an increasing trend in these constituents (Supplementary Table 2). Concentrations of bicarbonate decreased (negative slope with p-value < 0.05) in three of the twelve lysimeters. Sulfate concentrations decreased in two of the twelve lysimeters, with the remaining lysimeters exhibiting no significant trend. For Fe only one of the twelve lysimeters exhibits a statistically significant trend (p-value < 0.05) with the trend decreasing. Increases in K were clearly seen in a number of the lysimeters (5 of 12), while only one lysimeter exhibited a decreasing trend and the remaining six lysimeters did not exhibit any trend (i.e. slope estimate p-value > 0.05). Increases in phosphorus were similarly observed in many of the lysimeters (5 of 12) with the remaining lysimeters not exhibiting any significant trend. The majority of the lysimeters (10 of 12) exhibited no significant trend in arsenic concentrations, however statistically significant increasing trends were observed in two lysimeters. While As concentrations increased in these lysimeters between January 2012 and August 2017, the concentrations nonetheless remain at the relatively low levels of 13 ppb and 6 ppb (lysimeters 1–100 and 2–100 respectively).

It is worth noting that three shallowest lysimeter depths (0.25 m, 0.5 m, and 1 m) are located within the clay layer beneath the pond. Given that pond recharge largely bypasses the clay layer beneath the pond through burrows, these samples represent relatively slow flowing groundwater. The deeper samplers beneath the pond (≥1.5 m below the pond) largely reflects pond recharge that rapidly flowed down a preferential flow-path (crab burrow) and into the underlying sand/silt layer beneath the pond (Fig. 2 and Fig. 3).

4.2. Sediment inorganic geochemistry

X-ray diffraction analysis was performed on shallow sediments collected beneath our study pond nine months after the pond was constructed (Table 3). XRD detection limits for most mineral phases are greater than 1% by weight, so minor phases were not identified by XRD. There appears to be minimal depth variation in sediment mineralogy over the upper 1.3 m beneath the pond (2.1–3.4 m BLS), with quartz and muscovite/illite as the dominant phases and subordinate amounts of clinochlore/chlorite, albite (Na-plagioclase), and anorthite (Ca-plagioclase) (Table 3).

Our field site sits on the border of the Ganges River Floodplain and the Old Meghna Estuarine Floodplain units on the map of the physiographic units of Bangladesh (Brammer, 1996). The absence of smectite in the sediments at our field site suggest that the field area is part of the Old Meghna Estuarine Floodplain unit. Sediments from the Old Meghna Estuarine Floodplain are observed to have

Table 1
Mean geochemical parameters for pond water and shallow groundwater samples from beneath the pond (sample at 3.8 m BLS is not beneath the study pond). Depths are relative to pond bottom. Depths in parentheses are relative to land surface. The number of samples on which the mean was calculated are indicated by the "n" values in parenthesis; n.m. indicates "not measured". Standard deviations are shown in brackets.

Depth	**Sampling points**	**pH**	**Cond**	**DO**	**Alk**	**DIC**	**NH3-N**	**DOC**	**As**	**Sr**	**Si**	**Na**	**K**	**Mg**	**Ca**	**S**	**P**	**Fe**	**Mn**
m	*n*	-	*uS/cm*	*mM*	*mM* HCO_3	*mM*	*mM*	*mM*	*uM*	*uM*	*mM*	*mM*	*mM*	*mM*	*mM*	*mM*	*mM*	*mM*	*mM*
0 (Pond water)	1	7.35 [0.53] (n = 22)	217 [104] (n = 22)	0.156 [0.098] (n = 16)	1.76 [0.73] (n = 20)	2.03 [0.75] (n = 18)	0.01 [0.01] (n = 20)	0.33 [0.10] (n = 28)	0.08 [0.08] (n = 30)	0.95 [0.41] (n = 30)	0.10 [0.10] (n = 28)	0.24 [0.19] (n = 29)	0.047 [0.042] (n = 29)	0.28 [0.18] (n = 29)	0.58 [0.19] (n = 29)	0.13 [0.04] (n = 29)	0.001 [0.001] (n = 29)	0.003 [0.004] (n = 31)	0.001 [0.001] (n = 31)
0.25 (2.35)	3	7.10 [0.14] (n = 4)	501 [153] (n = 4)	*n.m.*	4.63 [1.08] (n = 15)	5.49 [1.51] (n = 4)	0.03 [0.02] (n = 15)	0.41 [0.23] (n = 26)	0.04 [0.03] (n = 22)	1.61 [0.45] (n = 27)	0.45 [0.09] (n = 27)	0.57 [0.19] (n = 30)	0.064 [0.024] (n = 30)	0.69 [0.20] (n = 30)	1.43 [0.43] (n = 30)	0.11 [0.06] (n = 30)	0.003 [0.008] (n = 30)	0.012 [0.013] (n = 30)	0.009 [0.006] (n = 30)
0.5 (2.6)	3	7.25 [0.29] (n = 6)	465 [118] (n = 7)	*n.m.*	4.71 [0.97] (n = 21)	5.34 [1.12] (n = 6)	0.03 [0.02] (n = 21)	0.48 [0.37] (n = 29)	0.03 [0.02] (n = 25)	1.63 [0.46] (n = 31)	0.45 [0.10] (n = 31)	0.59 [0.2] (n = 33)	0.063 [0.017] (n = 33)	0.70 [0.23] (n = 33)	1.45 [0.45] (n = 33)	0.11 [0.07] (n = 33)	0.002 [0.002] (n = 33)	0.018 [0.018] (n = 33)	0.011 [0.008] (n = 33)
1.0 (3.1)	3	7.07 [0.12] (n = 7)	525 [90] (n = 9)	*n.m.*	5.27 [0.59] (n = 20)	6.09 [0.91] (n = 7)	0.03 [0.02] (n = 19)	0.43 [0.34] (n = 28)	0.04 [0.03] (n = 24)	1.81 [0.28] (n = 29)	0.49 [0.07] (n = 29)	0.67 [0.12] (n = 32)	0.075 [0.032] (n = 32)	0.81 [0.16] (n = 32)	1.65 [0.28] (n = 32)	0.10 [0.06] (n = 32)	0.006 [0.009] (n = 32)	0.041 [0.03] (n = 32)	0.009 [0.003] (n = 32)
1.5 (3.6)	3	7.12 [0.15] (n = 8)	563 [69] (n = 8)	*n.m.*	5.30 [0.62] (n = 19)	6.19 [0.63] (n = 8)	0.04 [0.03] (n = 19)	0.55 [0.37] (n = 31)	0.03 [0.01] (n = 25)	1.91 [0.2] (n = 31)	0.53 [0.05] (n = 31)	0.71 [0.09] (n = 33)	0.071 [0.008] (n = 33)	0.87 [0.14] (n = 33)	1.72 [0.24] (n = 33)	0.10 [0.06] (n = 33)	0.005 [0.005] (n = 33)	0.053 [0.039] (n = 33)	0.009 [0.005] (n = 33)
3.81	1	6.81 [0.05] (n = 3)	679 [46] (n = 3)	0.015 (n = 1)	4.50 [0.77] (n = 2)	5.94 [1.22] (n = 2)	0.08 [0.00] (n = 2)	0.26 [0.07] (n = 4)	0.07 [0.03] (n = 3)	2.17 [0.04] (n = 3)	0.53 [0.05] (n = 3)	0.82 [0.01] (n = 3)	0.092 [0.038] (n = 3)	0.92 [0.09] (n = 3)	1.77 [0.11] (n = 3)	0.39 [0.06] (n = 3)	0.013 [0.004] (n = 3)	0.123 [0.094] (n = 3)	0.015 [0.007] (n = 3)
2.0 (4.1)	2	6.78 [0.07] (n = 6)	657 [30] (n = 6)	0.023 [0.026] (n = 2)	5.72 [0.75] (n = 6)	7.29 [0.92] (n = 4)	0.05 [0.02] (n = 4)	0.30 [0.05] (n = 12)	0.05 [0.01] (n = 12)	2.26 [0.16] (n = 12)	0.53 [0.07] (n = 12)	0.90 [0.33] (n = 12)	0.084 [0.007] (n = 12)	1.02 [0.09] (n = 12)	1.96 [0.17] (n = 12)	0.17 [0.06] (n = 12)	0.022 [0.008] (n = 12)	0.087 [0.033] (n = 12)	0.014 [0.004] (n = 12)
2.8 (4.9)	2	6.77 [0.04] (n = 6)	680 [39] (n = 6)	0.004 (n = 1)	5.41 [1.64] (n = 6)	7.79 [1.42] (n = 4)	0.05 [0.00] (n = 4)	0.28 [0.07] (n = 14)	0.05 [0.01] (n = 10)	2.38 [0.37] (n = 12)	0.51 [0.08] (n = 12)	0.86 [0.31] (n = 12)	0.093 [0.01] (n = 12)	1.01 [0.19] (n = 12)	1.97 [0.34] (n = 12)	0.17 [0.04] (n = 12)	0.027 [0.013] (n = 12)	0.073 [0.046] (n = 12)	0.014 [0.004] (n = 12)
3.5 (5.6)	2	6.78 [0.06] (n = 6)	668 [33] (n = 6)	0.002 (n = 1)	5.30 [1.37] (n = 6)	7.36 [1.49] (n = 4)	0.07 [0.02] (n = 4)	0.29 [0.05] (n = 12)	0.08 [0.01] (n = 12)	2.36 [0.31] (n = 12)	0.55 [0.07] (n = 12)	0.76 [0.11] (n = 12)	0.103 [0.013] (n = 12)	0.99 [0.15] (n = 12)	1.97 [0.27] (n = 12)	0.14 [0.03] (n = 12)	0.033 [0.008] (n = 12)	0.097 [0.02] (n = 12)	0.012 [0.003] (n = 12)

Table 2
Saturation indices of pond water and groundwater for selected set of minerals. Depths are relative to pond bottom. Depths in parentheses are relative to land surface, and a depth of zero represents pond water. SI is equal to the log(IAP/K_{eq}) except for CO_2(g) where it is equal to the log of the partial pressure in atmospheres.

Depth *(m)*	Calcite *SI*	Gypsum *SI*	Hydroxyapatite *SI*	Quartz *SI*	Rhodochrosite *SI*	Siderite *SI*	Vivianite *SI*	CO_2 (g) *SI*	CO_2 (g) *Atm*
0	−0.81	−2.89	−3.6	−0.07	−0.97	−0.71	−4.12	−2.23	0.006
0.25 (2.35)	−0.08	−2.66	−2.6	0.62	0.26	−0.05	−3.71	−1.68	0.021
0.5 (2.6)	0.07	−2.66	−1.88	0.61	0.43	0.23	−2.97	−1.8	0.016
1.0 (3.1)	−0.02	−2.68	−1.75	0.63	0.21	0.47	−1.75	−1.57	0.027
1.5 (3.6)	0.01	−2.67	−1.14	0.69	0.23	0.61	−0.97	−1.62	0.024

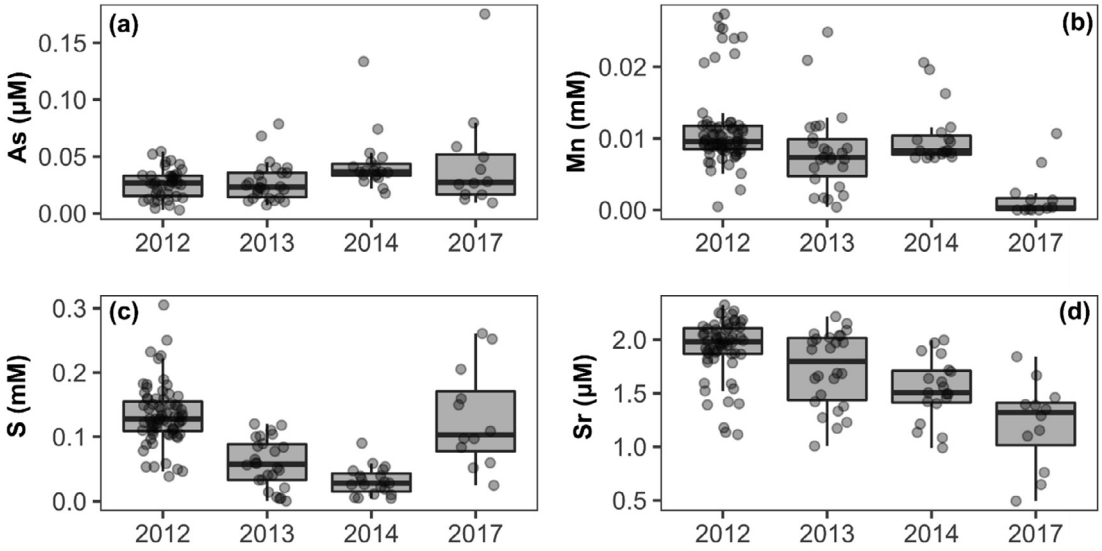

Fig. 4. Box plots of aqueous arsenic (a), manganese (b), sulfur (c), and strontium (d) in the shallow (0.25–1.5 m below the pond) groundwater beneath the pond. Samples are grouped by sampling year (no samples were collected in 2015 or 2016). Circles represent the individual samples and the box plots summarize the data within a given year. Note that concentrations of As (a) are very low well below WHO guidelines (0.13 µM) in all but two samples.

Table 3
Mineralogy of sediments beneath the study pond. Depths are relative to pond bottom and depths in parentheses are relative to land surface. Mineral phases shown within parentheses represent the clay form of the mineral. Uncertainty values represent two standard deviations of duplicate analysis and n.d. is non-detect.

Depth *m*	Clinochlore (Chlorite) *wt %*	Albite *wt %*	Anorthite *wt %*	Quartz *wt %*	Muscovite (illite) *wt %*	Montmorillonite (smectite) *wt %*
0.09 (2.19)	8.0	9.4	4.7	45.8	32.2	*n.d.*
1.3 (3.4)	7.8 ± 0.3	7.7 ± 1.3	4.4 ± 0.6	46.4 ± 2.7	33.8 ± 4	*n.d.*

minimal smectite whereas smectite is abundant within Ganges River Floodplain averaging approximately 40% by weight (Brammer, 1996; Heroy et al., 2003).

Elemental concentrations of the shallow sediments beneath our study pond were determined by X-ray fluorescence (XRF) and there appears to be little variation with depth over the sampled interval (Table 4). Consistent with the abundance of phyllosilicates (i.e., chlorite and muscovite/illite), tectosilicates (i.e., albite and anorthite) and quartz, we find silica and aluminum to be the dominant elements. Iron is the next most abundant element with concentrations above 4% and calcium, magnesium, and potassium concentrations all exceed 1% by weight. Subordinate amounts of sodium, titanium, phosphorus, manganese, and sulfur are also observed (Table 4).

4.3. Solid-phase and aqueous carbon pools below the pond

The solid-phase concentration of OC ranges between 0.27% and 0.57% by weight and is an order of magnitude greater than the solid-phase inorganic carbon (IC) which never exceeds 0.01% by weight (0.08% by weight as $CaCO_3$) (Table 5). The low solid-phase IC indicates that carbonate minerals are scarce within the sediments at our field site

Table 4
Elemental composition of sediments beneath the study pond. Depths are relative to pond bottom and depths in parenthesis are relative to land surface. Uncertainty values represent two standard deviations of duplicate analysis.

	Depth (m)	
	0.09 (2.19)	1.3 (3.4)
Na (wt %)	0.27	0.26 ± 0.06
Mg (wt %)	1.30	1.24 ± 0.04
Al (wt %)	8.63	8.34 ± 0.22
Si (wt %)	27.72	27.53 ± 0.66
P (wt %)	0.13	0.13 ± 0.00
K (wt %)	2.76	2.72 ± 0.02
Ca (wt %)	1.18	1.21 ± 0.02
Ti (wt %)	0.52	0.51 ± 0.02
Mn (wt %)	0.11	0.09 ± 0.00
Fe (wt %)	4.54	4.28 ± 0.00
S (wt %)	0.08	0.08 ± 0.00

and is consistent with the finding that sediments from the Old Meghna Estuarine Floodplain are non-calcareous (Brammer, 1996). Both the $\delta^{13}C$ and FM ^{14}C of the solid-phase IC differ greatly from that of the groundwater DIC – providing strong evidence that the small amount of solid-phase IC present is not from the precipitation of present-day DIC (Table 5).

The ages of the sediment IC and sediment OC are in close agreement and suggest that the shallow sediments at our field site were deposited in the mid-Holocene between 5 and 6 kyr BP (Fig. 2 and Table 5). Furthermore, the fact that the sediment IC has an age close to that of the sediment OC suggests that the IC precipitated at or near the time of deposition and is not composed of carbonate minerals that were eroded from FM ^{14}C dead rock formations upstream.

The ages of the DIC in the shallow groundwater beneath the pond are all less than 300 yrs BP and are much younger than the DOC found over the same depth interval, which have ages ranging from 775 to 2300 yrs BP (Fig. 2 and Table 6). The DOC in the pond water has an age of 520 ± 20 yrs BP and is younger than that of the groundwater DOC, suggesting that older sediment organic matter is released into solution as the pond water recharges the sediments and the resulting DOC is a mixture of OC with at least two different age signatures (Fig. 2, Table 5 and 6).

5. ANALYSIS AND DISCUSSION

5.1. Electron balance below the pond

5.1.1. Overview

It is widely agreed upon that oxidation of OC fuels the redox processes responsible for As mobilization in the aquifers of Bangladesh. Thus, quantification of the amount of OC oxidized as pond water flows through the shallow sediments is vital to understanding how ponds affect aquifer redox processes and As mobilization. Given that the oxidation of OC generates DIC, concentrations of DIC can provide insight into the amount of OC oxidation that has occurred. Our data clearly indicate that the oxidation of OC is the only significant source of DIC beneath the pond and that there are no significant sinks of DIC (see supplementary material for details) – thus observed changes in DIC with depth, when combined with flow rates, represent the amount of OC oxidized as pond water recharges the aquifer.

The mineralization of OC that we observe as pond water recharges the aquifer requires a terminal electron acceptor (TEA). Given the negligible amount of methanogenesis the vast majority (>99%) of the TEAs must be something other than the carbon itself (see supplementary materials). The anoxic conditions in the groundwater as indicated by the presence of dissolved Fe and Mn, further suggest that organic matter oxidation is the only electron donating process of significance within the aquifer (i.e., oxidation of Fe (II), Mn(II), sulfide is not occurring) (Appelo and Postma, 2010).

Given the importance of the reductive dissolution of As bearing iron-oxides for the release of As into groundwater, it is essential that we quantify the amount of reduction occurring, identify potential TEAs, determine the source of these TEAs and the rates at which they may be depleted. To address these questions we have constructed an electron budget for the shallow zone beneath the pond. We ultimately conclude the following:

1) The OC acting as the primary electron donor (ED) is sourced from an organic-rich 'pond muck' layer on or just below the pond bottom.
2) Pond derived OC is efficiently mineralized (>90%) after flowing into the shallow sediments (<1.5 m below the pond) and thus significant quantities are unlikely to be advected further into the aquifer.
3) The electron acceptors (EA) that are oxidizing the organic matter are largely (90%) sediment sourced.
4) The EAs appear to be iron oxides and sulfate and absent any re-oxidation these EAs could be annually depleted approximately 7 cm into the sediment under current conditions.
5) The vast majority (>99%) of the reduced iron and sulfate form secondary mineral phases and do not enter into solution.

5.1.2. Calculation of electron transfers

In this section, we use measured changes in aqueous geochemistry along a flow path to calculate the electron transfers that occur as pond water recharges the aquifer. For these calculations we use differences in chemistry between the pond water and the porewater samplers at 1.5 m below the pond (50 cm into the sand/silt) to calculate the electron transfers that occur during pond water recharge (Tables 7, 8, and 9). Given that crab burrows increase the hydraulic conductivity of the clay layer beneath the pond by a factor of at least 100, nearly all of the pond recharge bypasses the upper 1 m of clay as it flows through these burrows (Stahl et al., 2014). Therefore, the water at the top of the sand/silt layer represents pond water that was rapidly shunted down crab burrows to the sand/silt layer (Fig. 3) and groundwater at 1.5 m depth beneath the pond represents

Table 5
Abundances and stable isotopic composition for solid-phase organic and inorganic carbon. All samples were collected on sediments beneath the study pond. Depths are relative to pond bottom and depths in parenthesis are relative to land surface. Uncertainty values (except for OC and IC Fraction Modern) represent two standard deviations of duplicate analysis and n.m. indicates no measurement taken. Uncertainty values for OC and IC Fraction modern represent the analytical uncertainty.

Depth	TOC	δ^{13}C OC	TIC	δ^{13}C IC	OC Fraction Modern	OC Age	IC Fraction Modern	IC Age
m	*wt %*	*‰ VPDB*	*wt % as CaCO3*	*‰ VPDB*		*yr*		*yr*
0.06 (2.16)	0.41	−21.07	0.10	−5.1	*n.m.*	*n.m.*	0.5099 ± 0.0011	5410 ± 15
0.12 (2.23)	0.48 ± 0.04	−19.90 ± 0.06	0.05 ± 0.04	*n.m.*	0.4713 ± 0.0021	6040 ± 35	*n.m.*	*n.m.*
0.18 (2.29)	0.57	−18.27	0.08	*n.m.*	*n.m.*	*n.m.*	*n.m.*	*n.m.*
0.24 (2.35)	0.53	−17.90	0.08	*n.m.*	*n.m.*	*n.m.*	*n.m.*	*n.m.*
0.3 (2.41)	0.28	−19.01	0.05	*n.m.*	*n.m.*	*n.m.*	*n.m.*	*n.m.*
0.38 (2.48)	0.37	−21.10	0.05	*n.m.*	*n.m.*	*n.m.*	*n.m.*	*n.m.*
0.46 (2.56)	0.46	−18.67	0.06	*n.m.*	*n.m.*	*n.m.*	*n.m.*	*n.m.*
0.53 (2.64)	0.36 ± 0.08	−18.44 ± 0.04	0.05 ± 0.04	*n.m.*	*n.m.*	*n.m.*	*n.m.*	*n.m.*
0.61 (2.71)	0.43	−17.89	0.08	*n.m.*	*n.m.*	*n.m.*	*n.m.*	*n.m.*
1.3 (3.4)	0.55	−22.34	*n.m.*	*n.m.*	0.4760 ± 0.0020	5960 ± 35	*n.m.*	*n.m.*

the recharge water after it has flowed 50 cm into the sand/silt layer.

The electron transfers from the oxidation of organic matter (which acts as an ED) and the different TEA processes that we can infer from changes in aqueous chemistry as the pond water flows out of a crab burrow and then 50 cm into the sand/silt matrix are reported in Table 8 and Table 9 (see Table 7 for conversion from electron transfers per mole of compound oxidized/reduced). For all calculations in this section that require sediment grain density and/or porosity, we assume values of 2.65 g/cm^3 and 40% respectively.

Given that oxidation of OC is the only significant source of DIC beneath the pond and that there are no significant sinks of DIC – the observed changes in DIC that occur as pond water flows across the upper 50 cm of the sand/silt matrix (Fig. 2 and Fig. 3) beneath the pond provide an estimate of the total electrons donated in this depth interval. Eq. (5.1) shows the calculation of electrons transferred from the oxidation of OC

$$ED_{Tot} = EA_{Tot} = \left([DIC]_{GW} - [DIC]_{Pond}\right) \cdot EE_C \quad (5.1)$$

where all chemical species are in molar concentrations, with subscripts 'Pond' and 'GW' representing the average concentration measured on the inflowing pond water and the groundwater 1.5 m beneath the pond (50 cm into the sand/silt matrix) respectively, EE_C is the number of electrons transferred per mole of OC oxidized (i.e., 4 moles of electrons per mole of C oxidized), and ED_{Tot} is the number of electrons donated per unit volume of water. Each electron transferred must necessarily be accepted by a TEA (e.g., O_2, SO_4, Fe(III), Mn(IV),...) and thus our calculation of the total number of electrons donated during OC oxidation determines the total number of electrons accepted during OC oxidation as well (i.e. $ET_{Tot} = ED_{Tot} = EA_{Tot}$).

Table 9 shows the ED and EA required to produce the observed changes in aqueous chemistry as pond water flows through the upper 50 cm of the sand/silt sediment matrix as well as the ED (DOC) and EA (O_2, NO_3, and SO_4) available in the recharging pond water. Notably, the required electron donors (OC) and required electron acceptors greatly exceeds those available in the recharging pond water (i.e., pond water DOC and pond water O_2, NO_3 and SO_4) (Table 9),

5.1.3. Source of Electron Donors (ED) and Electron Acceptors (EA)

Since the oxidation of one mole of OC yields one mole of IC, less than 10% of the 4.2 mM increase in DIC that occurs as pond recharge flows 50 cm into the sand/silt sediment matrix could be explained by the average DOC concentration of 0.33 mM in the pond water (maximum DOC measured in the pond never exceeded 0.6 mM). Thus, there must be a solid-phase source of OC at or directly below the pond/burrow bottom-sediment interface, which is acting as the primary electron donor in the shallow sediment zone. Furthermore, DOC concentrations below this depth remain low (Fig. 2) indicating that if any of the solid-phase source of OC at or directly below the pond/burrow bottom-

Table 6
Radiocarbon dating of DOC and DIC on pond water and groundwater collected in the shallow aquifer. Depths are relative to pond bottom and depths in parenthesis are relative to land surface. Uncertainty represents analytical uncertainty.

2013 Samples

		Dissolved Organic Carbon (DOC)					Dissolved Inorganic Carbon (DIC)				
Sample ID	Depth	Age	FM	$\Delta^{14}C$	$\delta^{13}C$	DOC	Age	FM	$\Delta^{14}C$	$\delta^{13}C$	DIC
–	*m*	*yr*	–	*‰*	*‰ VPDB*	*mM*	*yr*	–	*‰*	*‰ VPDB*	*mM*
LYS1-150	1.5 (3.6)	1050 ± 25	0.8772 ± 0.003	−129.46	−26.15	0.283	*n.m.*	*n.m.*	*n.m.*	*n.m.*	*n.m.*
LYS2-150	1.5 (3.6)	1800 ± 25	0.7997 ± 0.0027	−206.37	−26.86	0.211	*n.m.*	*n.m.*	*n.m.*	*n.m.*	*n.m.*
SWC1-Y	2.8 (4.9)	905 ± 25	0.8935 ± 0.0028	−113.28	−26.55	0.192	45 ± 35	0.9942 ± 0.0042	−13.35	−17.98	9.22
SWC2-Y	2.8 (4.9)	955 ± 20	0.8878 ± 0.0025	−118.94	−26.64	0.207	290 ± 25	0.9647 ± 0.0033	−42.62	−16	8.02
PWC-20	4.0 (6.1)	775 ± 20	0.9079 ± 0.0024	−98.99	−26.23	0.243	255 ± 20	0.9688 ± 0.0024	−38.55	−16.56	7.67

2014 Samples

		Dissolved Organic Carbon (DOC)					Dissolved Inorganic Carbon (DIC)				
Sample ID	Depth	Age	FM	$\Delta^{14}C$	$\delta^{13}C$	DOC	Age	FM	$\Delta^{14}C$	$\delta^{13}C$	DIC
–	*m*	*yr*	–	*‰*	*‰ VPDB*	*mM*	*yr*	–	*‰*	*‰ VPDB*	*mM*
Pond	0	520 ± 20	0.9373 ± 0.0021	−69.9	−28.55	0.120	>Modern	1.0217 ± 0.0032	13.82	−13.08	1.51
LYS2-50	0.5 (2.6)	2300 ± 35	0.7509 ± 0.0032	−254.89	−27.7	0.153	*n.m.*	*n.m.*	*n.m.*	*n.m.*	*n.m.*
LYS2-150	1.5 (3.6)	905 ± 15	0.8934 ± 0.0019	−113.53	−32.74	0.441	*n.m.*	*n.m.*	*n.m.*	*n.m.*	*n.m.*
LYS3-150	1.5 (3.6)	1800 ± 25	0.7992 ± 0.0024	−207.01	−27.02	0.211	*n.m.*	*n.m.*	*n.m.*	*n.m.*	*n.m.*
SWC1-R	2.0 (4.1)	1020 ± 25	0.8811 ± 0.0025	−125.66	−26.68	0.214	180 ± 20	0.9776 ± 0.0023	−29.91	−16.17	7.41
SWC2-R	2.0 (4.1)	1130 ± 25	0.869 ± 0.0026	−137.72	−26.05	0.160	*n.m.*	*n.m.*	*n.m.*	*n.m.*	*n.m.*
SWC1-Y	2.8 (4.9)	895 ± 20	0.8947 ± 0.0025	−112.2	−26.77	0.181	25 ± 20	0.9969 ± 0.0023	−10.76	−16.89	7.07
PWC-20	4.0 (6.1)	810 ± 25	0.9039 ± 0.0026	−103.05	−26.01	0.249	270 ± 20	0.9668 ± 0.0024	−40.66	−16.93	7.73

Table 7
Redox reactions overview. Moles of each chemical species oxidized or reduced per mole of DIC generated and the moles of electrons donated (−) or accepted (+) are for each reaction are shown below.

Process	Reaction	mole X : mole DIC	Moles e : mole reacted
O_2 Red	O_2 to CO_2 (0 to -II)	1.3	+2
NO_3 Red	NO_3 to N_2 (V to 0)	0.8	+5
Mn Red	Mn(IV) to Mn(II)	2	+2
Fe Red	Fe(III) to Fe(II)	4	+1
SO_4 Red	SO_4 to S (VI to -II)	0.5	+8
Org. C Ox.	C(0) to C(IV)	1	−4

Table 8
Electron balance of recharge beneath study pond. C_{Pond} is inflowing pond water concentration (average value of pond water) and C_{GW} is the groundwater concentration at end of the flow-path under consideration (average value of groundwater 1.5 m beneath the pond). The electron transfers column shows the implied electron transfers from observed changes in aqueous chemistry (negative values for reduction and positive for oxidation).

Chem. Species –	C_{Pond} *mM*	C_{GW} *mM*	C_{Pond}-C_{GW} *mM*	Electron Transfers *meq/L*
Fe(II)	0.003	0.053	0.05	−0.05
Mn(II)	0.001	0.009	0.008	−0.016
SO_4	0.13	0.10	−0.03	−0.24
NO_3	0	0	0	0
O_2	0.156	0.023	−0.133	−0.532
DIC	2.03	6.19	4.16	16.64

Table 9
Required and available electron donors in the flow-path under consideration. The electron donors (ED) in the pond water is determined from the dissolved organic carbon concentration. The electron acceptors (EA) in the pond water is determined from the O_2, SO_4, and NO_3 in the pond water. The electron transfers that occur along the recharge flow-path is determined from the change in DIC along the flow-path (see Section 5.1)

	meq/L
ED in pond water	1.32
EA in pond water	1.66
EA transfers along recharge flow-path	16.64

sediment interface becomes DOC it is efficiently mineralized after flowing < 50 cm into the sediment matrix.

To identify the solid-phase OC source that is oxidized as pond recharge flows into the sediment matrix we calculated the age of the DIC generated within the shallow zone beneath the pond. The age of the generated DIC was calculated using Equation (5.2), which shows that the DIC $\Delta^{14}C$ of the shallow groundwater beneath the pond is the concentration weighted average of the $\Delta^{14}C$ of the DIC in the recharging pond water and the $\Delta^{14}C$ of the generated DIC.

$$\Delta 14C_{GW}^{DIC} = \Delta 14C_{Pond}^{DIC} \cdot \frac{[DIC]_{Pond}}{[DIC]_{GW}} + \Delta 14C_{Input}^{DIC} \cdot \frac{[DIC]_{Input}}{[DIC]_{GW}} \quad (5.2)$$

where, $[DIC]_{Input} = [DIC]_{GW} - [DIC]_{Pond}$

Substituting in the measured DIC concentrations and $\Delta^{14}C$ in the pond water and groundwater we solved for the $\Delta^{14}C$ of the generated DIC. We calculate that the age of the DIC generated as the pond water recharged the shallow sediments is 300 yrs BP, an age younger than the bulk DOC in pond water and groundwater and also younger than the sedimentary OC. It is important to note that this is an upper-bound (oldest potential age) for the age of the DIC generated. If there was any carbonate dissolution, which is at most a minor process (see supplementary material), the DIC input would have an old carbonate mineral component and the component from OC oxidation would be younger than the $\Delta^{14}C$ value calculated in Eq. (5.2). Thus, the calculated age of the DIC generated in the shallow zone beneath the pond clearly demonstrates that the bulk of the OC oxidized in this zone must be coming from a solid-source younger than both the sediment organic matter and the DOC measured in the groundwater beneath the pond. This young, solid-phase source of organic matter is likely algae, plant litter, and organic waste that settles to the bottom of the pond and forms a young, reactive, OC-rich layer which we refer to as 'pond muck'.

The existence of a layer of settled OC-rich material is a commonly observed feature in ponds and lakes throughout the world (Boyd, 1995; Kalff, 2002). Along with organic matter settling to the pond bottom, the roots of aquatic plants may also contribute young (i.e., ^{14}C modern) organic matter to the 'pond muck'. During the annual monsoon flooding aquatic plants (some of which are rooted) grow throughout our field area. While these plants are generally removed from pond areas prior to the recession of monsoon, it is likely that a substantial portion of root material is left behind in the shallow sediments of both pond and non-pond areas along with plant detritus that settles to pond bottoms. The root material thus provides a fresh source of young organic material to the shallow sediments

of both pond and non-pond areas each year. Another source of young organic matter that may contribute to the 'pond muck' is plant material carried by crabs into their burrows. Crabs found in the ponds and rice fields of the region are known to bring rice plants and other edible vegetation down into their burrows so that they can feed on the material within the safety of their burrows (Wagle, 1924; Stahl et al., 2014).

Moving past the upper 1.5 m beneath the pond (0.5 m into the sand/silt matrix, see Fig. 3), we observe much smaller changes with depth in DIC, indicating less redox activity in this zone (Fig. 2). At these depths we find DOC ages (775 to 2,300 yrs BP) that are significantly younger than the sedimentary OC (>5,900 yrs BP) and older than both the presumed bulk age of the "pond muck" (300 yrs BP) and surface water DOC (520 yrs BP) (Tables 5 and 6). Thus, the DOC at these depths is a mixture of sedimentary and surface-derived OC. Unlike in the upper 1.5 m zone beneath the pond where we observed the mineralization of a large quantity of young OC, here we observe significantly less mineralization of OC. Therefore, our findings indicate that reactive OC from the surface may be largely mineralized over short distances (<50 cm) into the sediment matrix, leaving a more limited quantity available to react at greater depths.

Just as the aqueous EDs in the pond water can only account for less than 10% of the EDs oxidized, the aqueous EAs in the pond water, the majority of which is sulfate (Table 8), could oxidize only 10% of the OC mineralized as pond recharge flows 50 cm into the sediment matrix (Table 9). Thus, solid-phase sources of EAs must be the primary oxidants in the shallow sediments beneath the pond. The solid-phase electron acceptors present in the sediments at our site (both beneath the pond and deeper into the sediments) likely consist of iron and manganese oxides and ferric clay minerals. We measure substantial solid-phase concentrations of iron and manganese along with subordinate amount of solid-phase sulfur (Table 4), though we did not determine their speciation. However, mixed valence, iron-rich coatings on quartz, feldspar, and aluminosilicate minerals were widely observed on sediments from the upper 30 m of the aquifer at our site (Swartz et al., 2004). Polizzotto et al. (2006) performed quantitative XANES and EXAFS analysis of sediments from 5 m and 60 m depth at our field site and determined that all of the Fe(III) in these sediment samples could be accounted for in aluminosilicates and magnetite . Therefore, these phases may be acting as TEAs for the oxidation of OC. Phyllosilicate minerals containing structural ferric iron are another possible source of electron acceptors within the sediments. Structural ferric iron is commonly observed in phyllosilicates and microbial respiration of this Fe(III) source has been widely demonstrated for a range of different phyllosilicates, including chlorite and illite (Kostka et al., 1999; Fredrickson et al., 2003; Jaisi et al., 2007; Wu et al., 2012) which are abundant in our sediments (Table 3). While we did not measure the arsenic content of iron-bearing phyllosilicates for this study, other researchers working in the Bengal Delta have found that these phases, in particular biotite and chlorite, often host significant quantities of arsenic and act as sources of arsenic to the groundwater (Desbarats et al., 2017; Seddique et al., 2008, 2011).

The observed increase in aqueous iron and manganese as water recharges the aquifer (Table 1) provides a strong indication that iron and manganese reduction is occurring. Based on measured solid-phase concentrations of potential EAs and changes in aqueous chemistry as pond water recharges we calculate that the simultaneous reduction of sedimentary Fe(III), Mn(IV), and sulfate would annually result in the depletion of these three EAs approximately 7 cm into the sediment matrix (Table 10, see detailed discussion of calculations in the supplementary material). This calculation corroborates that there is ample sedimentary supply of EAs to oxidize OC to the observed levels of DIC found 50 cm into the sand/silt sediment matrix (Figs. 2, 3). Once the sedimentary electron acceptors are depleted over an interval, then the OC at that depth can be oxidized by any available aqueous electron acceptors in the recharge water or can be mineralized via methanogenesis. Thus, is it potentially the case that over time an increasing fraction of the labile organic matter that is sourced from the pond bottom may be mineralized via methanogenesis.

From our electron transfer calculations we have seen that the TEAs responsible for the oxidation of OC to DIC must be predominantly sediment sourced. We also find that the observed aqueous concentration of Fe(II), Mn (IV), and S(-II) (Table 8) are much lower than the concentrations expected based on our electron transfer calculations. This result indicates that the reduced species are precipitating into new mineral phases following reduction and that less than 1% of the reduced forms of the TEAs are entering into solution. Our observation of aqueous concentrations of reduced species well below values expected from the measured amount of OC oxidation is not anomalous and is often observed in groundwater systems (Chapelle, 1993; Park et al., 2006). A detailed discussion of solid-phase sinks for the reduced EAs is presented in the supplementary material and indicates that the observed aqueous concentrations beneath the pond are consistent with the estimated levels of Fe and or sulfate reduction required to drive the observed increases in DIC.

5.2. Role of man-made ponds in arsenic mobilization

Our electron balance and carbon mass balance calculations demonstrate that as pond water recharges, a large quantity (>4 mM) of the young labile OC carried in this recharge is mineralized in the shallow sediment zone. The vast majority of this mineralization appears to occur as pond recharge flows out of preferential flow-paths (crab burrow that bypasses the clay) reaching the sand/silt layer 50 cm beneath the pond (Fig. 2 and Fig. 3). The mineralization of OC is indicated by the large increase in DIC between the pond water and the water at 1.5 m depth beneath the pond, followed by only slight increases further into the underlying sediments. Furthermore, our results indicate it is unlikely that significant quantities of this labile OC have been advected deeper into the sediments beneath the pond as DOC concentrations are not particularly elevated in the upper few meters beneath the pond (Fig. 2). We also

find that the oxidation of this organic matter (methanogenesis was not a major mineralization pathway) is likely coupled to the reduction of sedimentary Fe (III) and aqueous sulfate (dissolved and potentially some sulfate sourced from organic matter, e.g., Schroth et al., 2007).

Prior research at our field site revealed a bell-shaped depth profile in groundwater As, with concentrations increasing from typically low levels (<50 μg/L) in the upper 10 m of the aquifer then peaking at levels often in excess of 500 μg/L around 30 m depth before dropping back down below 50 μg/L at 75 m depth (Swartz et al., 2004; Harvey et al., 2006; Neumann et al., 2010; Hug et al., 2011). Neumann et al. (2010) presented modeling evidence showing that the proportion of groundwater derived from pond recharge exhibits a very similar depth pattern to dissolved As and describes a nearby pond (~200 m from our study pond), which based on historical records is known to have been present for over 200 years (Neumann et al., 2014). Based on this evidence as well as concentration patterns in conservative groundwater tracers, Neumann et al. (2010) argued that pond recharge likely drives As mobilization and that the depth patterns in dissolved As are explained by the proportion of pond recharge at a given depth. However, the conclusions of Neumann et al. (2010) have been challenged by McArthur et al. (2011), who argued that recharge is not driving As mobilization and is instead flushing the shallow aquifer of As.

The results of this study suggest that recharge from recently constructed ponds may not be responsible for the patterns of groundwater As observed at our field site. While we observe reducing conditions and significant redox activity in the shallow sediments beneath our study pond, during the six years of our investigation, we have yet to observe any large changes in aqueous As concentrations beneath the pond (Fig. 4). Thus over the six years of this study the pond has not generated a recharge plume of high groundwater As. The majority (10 of 12) lysimeters beneath the study pond do not exhibit a statistically significant change in As concentrations (Supplementary Table 2) indicating that As levels beneath the pond have yet to respond to the influx of pond recharge. In addition, all of the lysimeters remain relatively low in arsenic, with 11 out of 12 lysimeters having As concentrations < 6 ppb and the remaining lysimeter < 13 ppb As.

While there is significant mineralization of OC as pond water flows through the shallow sediments beneath the pond, DOC concentrations beneath the pond indicate that significant quantities of this labile OC have not been advected past these shallow depths (Fig. 2). It may be the case, as Mailloux et al. (2013) argued using radiocarbon dates of microbial DNA, that OC introduced with aquifer recharge is retarded relative to groundwater flow and takes more than 1000 years to reach the depths where we observe high levels of As. While these findings do not preclude a role for aquifer recharge in the observed patterns of dissolved As, they would preclude OC from man-made ponds, which have only existed in large number for <70 years (Kränzlin, 2000), as a factor in As concentrations at depth.

Our results also suggest that the relatively labile nature of the OC mineralized beneath the pond, which is indicated by the large increases in DIC with minimal accumulation of DOC, may limit the advection of pond derived OC deep into the aquifer as it will be quickly mineralized in the shallow sediments. Depletion of TEAs in the shallow sediments beneath the pond should not affect rates of OC mineralization as the fermentative step, which produces fermentative intermediates (e.g., acetate, formate, H_2) is the rate limiting step, not the terminal electron accepting step (Middelburg, 1989; Boudreau and Ruddick, 1991; Appelo and Postma, 2010). Thus, the potential for pond derived OC to drive the reduction of sedimentary TEAs and As mobilization at depth within the aquifer may be limited by its labile nature which results in its mineralization before it can be advected far into the aquifer, resulting in only a narrow band of sediments beneath the pond depleted in sedimentary TEAs because the highly reactive OC is efficiently consumed prior to flowing through this depth interval.

We find that the shallow groundwater beneath our pond, which was recharged by pond water (see Sections 2.1–2.2 and supplementary material for discussion of hydrology), has chemistry that is similar to shallow groundwater recharged by rice fields (Table 1). This indicates that aquifer sediments as opposed to recharge source are likely the dominant first-order control on the groundwater chemistry. Neumann et al. (2011) found that the bulk of the OC mineralization (and DIC generation) that occurs as water recharges from rice fields, occurs in the upper 2 m of sediments and that the timing of rice field recharge limits the transport of reactive organic carbon into the subsurface. Furthermore, Neumann et al. (2011) observed that the majority of rice field recharge moves through macropores in the unplowed bunds (raised perimeter around rice fields) and that due to active photosynthesis in the fields the rice field water was often supersaturated with oxygen prior to entering the bunds. These characteristics of rice field recharge and the fact that rice fields maintain their sorptive capacity by desaturating periodically, which oxidizes the bunds and underlying sediments down to depths of >2 m following the annual rice harvest, led Neumann et al. (2011) to conclude that rice fields have limited potential for arsenic mobilization. We also find that much of the OC mineralization and DIC generation that occurs during pond recharge occurs after flowing through <2 m of sediment. While ponds typically do not dry out and experience re-oxidation of their underlying sediment, the relatively labile nature of the OC mineralized beneath the pond likely limits the reduction of sedimentary TEAs to a narrow band beneath the pond and thus may limit the potential for ponds recharge to generate high levels of groundwater As. The results from our study pond taken in consideration with the results of Neumann et al. (2011) on rice fields at our site, suggest that the geochemistry of the groundwater and the potential for arsenic mobilization at depth may be largely controlled by sediment (solid-phase) characteristics rather than recharge source – a conclusion that is consistent with our overall findings that the pond has not generated a plume of high As.

Our findings indicate that, because of the labile nature of the OC and/or retardation as suggested by Mailloux et al. (2013), the relatively recent introduction of widespread

Table 10
Electron balance for solid-phase constituents. Calculations of table values is described in Section 5.1 and supplementary Section 1.5. Sediment concentrations for Fe(III), Mn(IV), and SO_4 are described in supplementary Section 1.5 and sediment concentration for organic carbon is the average of the sediment organic carbon data reported in Table 5.

	Sediment Source Required *mg/g*	Aqueous Equivalent *mM*	Sediment Concentration *mg/g*	Pore Vol. to Deplete *num. vol.*	Depth Depleted Annually *m*
Fe(III)	0.210	14.98	4.56	22	0.26
Mn(IV)	0.103	7.49	0.90	9	0.64
SO_4	0.045	1.87	2.31	51	0.11
Fe(III), Mn(IV), and SO_4	–	–	–	81	0.07
Org C	0.012	3.83	4.30	371	0.015

man-made ponds (<70 years) is unlikely to have contributed significant quantities of OC to depths where we observe high levels of dissolved As. However, if man-made ponds do mobilize As from their shallow sediments over longer time scales, they could generate plumes of high As that could be advected deeper into the aquifer, similar to what has been observed with recharge from oxbow lakes in Cambodia and river recharge in Vietnam (Polizzotto et al., 2008; Stahl et al., 2016). Given that high concentrations of As were not generated beneath the pond over the time-scale of this experiment (>6 years) we need to examine whether man-made ponds may be expected to generate high As plumes over longer time-scales, in order to determine if man-made ponds have influenced presently observed conditions or if they will influence future conditions.

While man-made ponds in the Bengal Basin may seem to represent recharge environments similar to natural oxbow lakes and river banks, settings where high As recharge plumes have been observed, there are important differences that may greatly slow the development of high As plumes from ponds. At our field site and in Bangladesh in general, ponds are constructed by excavating the upper few meters of the sediment to create a depression in the land surface that subsequently fills with water. This construction method effectively removes the youngest sediments, and based on carbon dating of the sedimentary OC and IC, we find that the sediments in the upper 12 cm beneath our study pond (2.2 m BLS) are at least 5.4 kyr old (Table 5), and are therefore close to the age of the aquifer sediments which are likely Holocene down to ~100 m depth (Swartz et al., 2004). However, beneath oxbow lakes where plumes of high As have been observed, the underlying sediments are much younger than those found beneath our pond because sediment accumulates in oxbows. Polizzotto et al. (2008) found that the sediments 10 cm beneath a naturally formed flooded oxbow pond, which generates high As recharge, had a modern $\Delta^{14}C$ age and sediment ages <2 kyr were found to depths of 2 m below the oxbow pond bottom; ages that are much younger than the 6–7 kyr old aquifer (Kocar et al., 2008).

The rate of As release is observed to scale with the inverse of the sediment age (Postma et al., 2012; Stahl et al., 2016) and thus it is not surprising that recharge from the oxbow ponds at the Cambodia site of Polizzotto et al. (2008) generate higher As concentrations than the man-made ponds at our site (Fig. 5). The estimated rates of arsenic release beneath our study pond are consistent with what would be expected based on the sediment age (Fig. 5). The lower rates of arsenic release beneath our study pond relative to wetlands in Cambodia (Polizzotto et al., 2008) and riverbank sediments in Vietnam (Stahl et al., 2016) are likely explained by the much older sediment beneath the excavated man-made pond (Fig. 5). Furthermore, while our pond bottom sediments are receiving young labile OC (i.e., the pond muck that settles on the pond bottom), this labile source of OC must be advected through the sediments to drive the reduction of sedimentary TEAs. As discussed earlier the labile OC is mineralized over a very short distance (~50 cm) into the sediment matrix and thus its ability to generate an ever growing band of reduced sediments is likely limited.

Our findings suggest that As mobilization as a result of pond recharge may be largely confined to a relatively thin band (10's of cm) of reduced sediments beneath these ponds over decadal timescales, limiting their potential for generating plumes of high As. This differs from the shallow sediments beneath the oxbow ponds/wetlands at the site of Polizzotto et al. (2008) where the young organic matter was co-deposited with the sediments (which are also young) and can drive the reduction of sedimentary TEAs in-situ. Thus, the natural ponds/wetlands at the site of Polizzotto et al. (2008) are more similar to the very young (years to decades old) freshly deposited riverbed sediment found in Vietnam which exhibit rapid rates of As release (Stahl et al., 2016) than they are to the man-made ponds found at our field site. However, it is important to note that naturally occurring ponds at our site may behave similar to the natural ponds/wetlands described by Polizzotto et al. (2008). Thus, naturally occurring ponds due to their younger and likely more reactive bottom sediments, along with the fact that they would have existed over much longer time-scales than man-made ponds (whose presence was not significant until ~70 yrs ago) may have a more significant role in high groundwater As in Bangladesh than man-made ponds.

It is worth noting that geologic/geomorphic differences across the Bengal Basin are observed to affect aquifer geochemistry and As occurrence (e.g., Bhowmick et al., 2013;

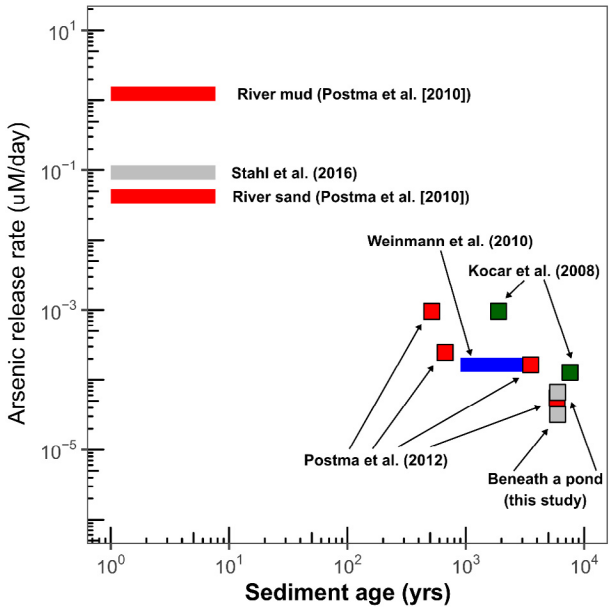

Fig. 5. The rate of arsenic release versus sediment age from beneath the man-made pond described in this study (gray squares); in aquifers around Hanoi, Vietnam (red squares); in an aquifer in Van Phuc, Vietnam (blue bar); in an aquifer in Cambodia (green squares); in riverbank sediments in Van Phuc, Vietnam (gray bar); from laboratory incubation experiments on river sediments from Vietnam (red bars). Details on the rate calculations and sediment ages are in provided in the Supplementary Material. (For interpretation of the references to colour in this figure legend, the reader is referred to the web version of this article.)

Mukherjee et al., 2018) and thus may also influence the impact of ponds on groundwater conditions. While the excavation of our study pond removed the young and likely reactive surficial sediments leaving only relatively aged (>5 kyr) sediments underneath (Table 5), this may not be the case for all man-made ponds. In areas where pond excavation is very shallow and/or areas with thick surface sequences of recently deposited sediments, man-made ponds may be underlain by young and reactive sediments. In these cases man-made ponds may play a role more similar to the natural ponds/wetlands that have been implicated in driving As mobilization (Polizzotto et al., 2008). Similarly, man-made ponds that have experienced significant infilling post-construction (e.g., decades old ponds in areas with high rates of deposition) may accumulate young reactive sediments on their bottom and begin to behave more like natural pond/wetlands (Neumann et al., 2010). Conversely, in some regions man-made ponds contribute much less recharge (Sengupta et al., 2008) than the man-made ponds at our field site, possibly due to thicker surficial clays, and thus their influence on the underlying groundwater may be limited. Given the potential role of geologic and geomorphic conditions on a pond's impact on groundwater As, future research examining these effects is merited. Nonetheless, our findings indicate that where the excavation of man-made ponds leaves only aged (i.e., thousands of years old) sediment beneath a pond, a pond's potential to mobilize As may be limited. While data on near surface sediment ages in the Bengal Basin is limited, Uddin and Abdullah (2003) report sediment ages in excess of 5 kyr at depths of 2 m below the land surface, which is similar to what we find at our site (Table 5) and suggests that excavation of man-made ponds elsewhere in the Bengal Basin may remove young reactive sediments and thereby limit the pond's potential to drive As mobilization.

6. CONCLUSIONS

While constructed ponds are known to have significantly changed the patterns and quantities of recharge in Bangladesh, and have been suggested to drive As mobilization (Harvey et al., 2002, 2006; Neumann et al., 2010), our study is the first to directly describe the geochemical processes that occur following the construction of a new man-made pond and to track these processes through time. Based on an electron balance, we have identified a set of likely terminal electron accepting (Fe and S reduction) and electron donating reactions (oxidation of OM largely sourced by pond muck) that occur beneath man-made ponds. Furthermore, we have provided quantitative evidence for solid-phase sources supplying the majority of both the electron acceptors and donors. We found that the organic matter introduced by the study pond is efficiently mineralized at shallow depths beneath the pond. This suggests organic carbon derived from man-made ponds is unlikely to be advected deeper into the aquifer and drive As mobilization over the depths where high levels of dissolved As are observed.

Over the six years of the study we did not observe any significant changes in aqueous As beneath the pond. Our results suggest that the excavation of man-made ponds, which removes young and reactive surficial sediments, may serve to limit their ability to generate high levels of As. Thus, man-made ponds stand in contrast to recharge settings such as riverbanks in Vietnam (Stahl et al., 2016) and oxbow ponds in Cambodia (Polizzotto et al., 2008; Stuckey et al., 2016), where young and reactive surficial sediments have not been removed and high concentrations of As have been observed.

Declaration of Competing Interest

The authors declare that they have no known competing financial interests or personal relationships that could have appeared to influence the work reported in this paper.

ACKNOWLEDGEMENTS

This work was supported by NIH P42ES016454, a NSF Graduate Research Fellowship and the Singapore National Research Foundation (NRF) through the Singapore-MIT Alliance for Research and Technology (SMART) Center for Environmental Sensing and Monitoring (CENSAM). We thank Laure Gandois and Britt Huhmann for assistance in the field; Kelly Whaley-Martin for measuring methane concentrations on several groundwater samples; Anis at BUET and the people of Bashailbhog village, most notably Sojib Chowdhury, Sha'alam, and Liton for their support of our project. We thank Rebecca Neumann for her valuable input and edits during the drafting of this manuscript.

All of the data associated with this manuscript are provided in the in-text tables, the supplementary material, and accompanying supplementary spreadsheet file.

APPENDIX A. SUPPLEMENTARY MATERIAL

Supplementary data to this article can be found online at https://doi.org/10.1016/j.gca.2020.08.012.

REFERENCES

Appelo C. A. and Postma D. (2010) *Geochemistry, groundwater and pollution*, 2nd ed. CRC Press, Boca Raton.

Argos M., Kalra T., Rathouz P. J., Chen Y., Pierce B., Parvez F., Islam T., Ahmed A., Rakibuz-Zaman M., Hasan R., Sarwar G., Slavkovich V., van Geen A., Graziano J. and Ahsan H. (2010) Arsenic exposure from drinking water, and all-cause and chronic-disease mortalities in Bangladesh (HEALS): a prospective cohort study. *Lancet* **376**, 252–258.

Beaupré S. R., Druffel E. R. M. and Griffin S. (2007) A low-blank photochemical extraction system for concentration and isotopic analyses of marine dissolved organic carbon. *Limnol. Oceanogr. Methods* **5**, 174–184.

Belton B. and Azad A. (2012) The characteristics and status of pond aquaculture in Bangladesh. *Aquaculture* **359**, 196–204.

BGS and DPHE (2001) Arsenic contamination of groundwater in Bangladesh. In *Hydrochemical Atlas. In British Geological Survey Report; WC/09/19*, vol. 3 (eds. D. G. Kinniburgh and P. L. Smedley). British Geological Survey, Keyworth, U.K.

Bhowmick S., Nath B., Halder D., Biswas A., Majumder S., Mondal P., Chakraborty S., Nriagu J., Bhattacharya P., Iglesias M., Roman-Ross G., Guha M. D., Bundschuh J. and Chatterjee D. (2013) Arsenic mobilization in the aquifers of three physiographic settings of West Bengal, India: Understanding geogenic and anthropogenic influences. *J. Hazard. Mater.* **262**, 915–923.

Boudreau B. P. and Ruddick B. R. (1991) On a reactive continuum representation of organic-matter diagenesis. *Am. J. Sci.* **291**, 507–538.

Boyd C. (1995) *Bottom soils, sediment, and pond aquaculture*. Springer.

Brammer H. (1996) *The geography of soils of Bangladesh*. The University Press Limited, Dhaka.

Chapelle F. H. (1993) *Ground-water microbiology and geochemistry*. John Wiley & Sons, New York.

Datta S., Neal A. W., Mohajerin T. J., Ocheltree T., Rosenheim B. E., White C. D. and Johannesson K. H. (2011) Perennial ponds are not an important source of water or dissolved organic matter to groundwaters with high arsenic concentrations in West Bengal, India. *Geophys. Res. Lett.* **38**, 1–5.

Desbarats A. J., Koenig C. E. M., Pal T., Mukherjee P. K. and Beckie R. D. (2014) Groundwater flow dynamics and arsenic source characterization in an aquifer system of West Bengal, India. *Water Resour. Res.* **50**, 4974–5002.

Desbarats A. J., Pal T., Mukherjee P. K. and Beckie R. D. (2017) Geochemical evolution of groundwater flowing through arsenic source sediments in an aquifer system of West Bengal, India. *Water Resour. Res.* **53**, 8715–8735.

Dittmar J., Voegelin A., Roberts L. C., Hug S. J., Saha G. C., Ali M. A., Badruzzaman A. B. M. and Kretzschmar R. (2007) Spatial distribution and temporal variability of arsenic in irrigated rice fields in Bangladesh. 2. Paddy Soil. *Environ. Sci. Technol.* **41**, 5967–5972.

Dowling C. B., Poreda R. J. and Basu A. R. (2003) The groundwater geochemistry of the Bengal Basin: Weathering, chemsorption, and trace metal flux to the oceans. *Geochim. Cosmochim. Acta* **67**, 2117–2136.

Downs R. T. and Hall-Wallace M. (2003) The American Mineralogist crystal structure database. *Am. Mineral.* **88**, 247–250.

Fredrickson J. K., Zachara J. M., Kennedy D. W. and Andarithes H. M. K. (2003) Microbial Reduction of Structural Fe (III) in Illite and Goethite. *Environ. Sci. Technol.* **37**, 1268–1276.

Harvey C. F., Swartz C. H., Badruzzaman A. B. M., Keon-Blute N., Yu W., Ali M. A., Jay J., Beckie R., Niedan V., Brabander D., Oates P. M., Ashfaque K. N., Islam S., Hemond H. F. and Ahmed M. F. (2002) Arsenic mobility and groundwater extraction in Bangladesh. *Science* **298**, 1602–1606.

Harvey C. F., Ashfaque K. N., Yu W., Badruzzaman A. B. M., Ali M. A., Oates P. M., Michael H. A., Neumann R. B., Beckie R., Islam S. and Ahmed M. F. (2006) Groundwater dynamics and arsenic contamination in Bangladesh. *Chem. Geol.* **228**, 112–136.

Heroy D., Kuehl, Jr., S. and Goodbred S. (2003) Mineralogy of the Ganges and Brahmaputra Rivers: implications for river switching and Late Quaternary climate change. *Sediment. Geol.* **155**, 343–359.

Horneman A., van Geen A., Kent D. V., Mathe P. E., Zheng Y., Dhar R. K., O'Connell S., Hoque M. A., Aziz Z., Shamsudduha M., Seddique A. A. and Ahmed K. M. (2004) Decoupling of As and Fe release to Bangladesh groundwater under reducing conditions. Part I: Evidence from sediment profiles. *Geochim. Cosmochim. Acta* **68**, 3459–3473.

Hug S. J., Gaertner D., Roberts L. C., Schirmer M., Ruettimann T., Rosenberg T. M., Badruzzaman A. B. M. and Ashraf Ali M. (2011) Avoiding high concentrations of arsenic, manganese and salinity in deep tubewells in Munshiganj District, Bangladesh. *Appl. Geochem.* **26**, 1077–1085.

Jaisi D. P., Dong H. and Liu C. (2007) Influence of biogenic Fe(II) on the extent of microbial reduction of Fe(III) in clay minerals nontronite, illite, and chlorite. *Geochim. Cosmochim. Acta* **71**, 1145–1158.

Jakobsen R., Kazmierczak J., Sø H. U. and Postma D. (2018) Spatial variability of groundwater arsenic concentration as controlled by hydrogeology: conceptual analysis Using 2-D reactive transport modeling. *Water Resour. Res.* **54**, 10254–10269.

Johnson J., Anderson G. and Parkhurst D. L. (2000) Database thermo. com. V8. R6. 230.

Kalff J. (2002) *Limnology*. Prentice Hall, Saddle River.

Klump S., Kipfer R., Cirpka O. A., Harvey C. F., Brennwald M. S., Ashfaque K. N., Badruzzaman A. B. M., Hug S. J. and Imboden D. M. (2006) Groundwater dynamics and arsenic mobilization in Bangladesh assessed using noble gases and tritium. *Environ. Sci. Technol.* **40**, 243–250.

Kocar B. D., Polizzotto M. L., Benner S. G., Ying S. C., Ung M., Ouch K., Samreth S., Suy B., Phan K., Sampson M. and Fendorf S. (2008) Integrated biogeochemical and hydrologic processes driving arsenic release from shallow sediments to groundwaters of the Mekong delta. *Appl. Geochem.* **23**, 3059–3071.

Kostka J. E., Haefele E., Viehweger R. and Stucki J. W. (1999) Respiration and dissolution of iron(III) containing clay minerals by bacteria. *Environ. Sci. Technol.* **33**, 3127–3133.

Kränzlin I. (2000) Pond management in rural Bangladesh: system changes, problems and prospects, and implication for sustainable development, Ph.D. Thesis, Basel University: Switzerland, pp. 213.

Lawson M., Polya D. A., Boyce A. J., Bryant C., Mondal D., Shantz A. and Ballentine C. J. (2013) Pond-derived organic

carbon driving changes in arsenic hazard found in asian groundwaters. *Environ. Sci. Technol.* **47**, 7085–7094.

Lawson M., Polya D. A., Boyce A. J., Bryant C. and Ballentine C. J. (2016) Tracing organic matter composition and distribution and its role on arsenic release in shallow Cambodian groundwaters. *Geochim. Cosmochim. Acta* **178**, 160–177.

Mailloux B. J., Trembath-Reichert E., Cheung J., Watson M., Stute M., Freyer G. A., Ferguson A. S., Ahmed K. M., Alam M. J., Buchholz B. A., Thomas J., Layton A. C., Zheng Y., Bostick B. C. and van Geen A. (2013) Advection of surface-derived organic carbon fuels microbial reduction in Bangladesh groundwater. *Proc. Natl. Acad. Sci.* **110**, 5331–5335.

McArthur J. M., Ravenscroft P., Safiulla S. and Thirlwall M. F. (2001) Arsenic in groundwater: Testing pollution mechanisms for sedimentary aquifers in Bangladesh. *Water Resour. Res.* **37**, 109–117.

McArthur J. M., Banerjee D., Hudson-Edwards K., Mishra R., Purohit R., Ravenscroft P., Cronin A., Howarth R., Chatterjee A., Talukder T., Lowry D., Houghton S. and Chadha D. (2004) Natural organic matter in sedimentary basins and its relation to arsenic in anoxic ground water: the example of West Bengal and its worldwide implications. *Appl. Geochem.* **19**, 1255–1293.

McArthur J. M., Ravenscroft P. and Sracek O. (2011) Aquifer arsenic source. *Nat. Geosci.* **4**(10), 655–656.

Middelburg J. J. (1989) A simple rate model for organic matter decomposition in marine sediments. *Geochim. Cosmochim. Acta* **53**, 1577–1581.

Mladenov N., Zheng Y., Miller M. P., Nemergut D. R., Legg T., Simone B., Hageman C., Rahman M. M., Ahmed K. M. and Mcknight D. M. (2010) Dissolved organic matter sources and consequences for iron and arsenic mobilization in Bangladesh aquifers. *Environ. Sci. Technol.* **44**, 123–128.

Mukherjee A., Fryar A. E., Eastridge E. M., Nally R. S., Chakraborty M. and Scanlon B. R. (2018) Controls on high and low groundwater arsenic on the opposite banks of the lower reaches of River Ganges, Bengal basin, India. *Sci. Total Environ.* **645**, 1371–1387.

Neumann R. B., Polizzotto M. L., Badruzzaman A. B. M., Ali M. A., Zhang Z. and Harvey C. F. (2009) Hydrology of a groundwater-irrigated rice field in Bangladesh: Seasonal and daily mechanisms of infiltration. *Water Resour. Res.* **45**, 1–14.

Neumann R. B., Ashfaque K. N., Badruzzaman A. B. M., Ashraf Ali M., Shoemaker J. K. and Harvey C. F. (2010) Anthropogenic influences on groundwater arsenic concentrations in Bangladesh. *Nat. Geosci.* **3**, 46–52.

Neumann R. B., St Vincent A. P., Roberts L. C., Badruzzaman A. B. M., Ali M. A. and Harvey C. F. (2011) Rice field geochemistry and hydrology: an explanation for why groundwater irrigated fields in Bangladesh are net sinks of arsenic from groundwater. *Environ. Sci. Technol.* **45**, 2072–2078.

Neumann R. B., Pracht L. E., Polizzotto M. L., Badruzzaman A. B. M. and Ali M. A. (2014) Biodegradable organic carbon in sediments of an arsenic-contaminated aquifer in Bangladesh. *Environ. Sci. Technol. Lett.* **1**, 221–225.

Nghiem A. A., Stahl M. O., Mailloux B. J., Mai T. T., Trang P. T., Viet P. H., Harvey C. F., Geen A. and Bostick B. C. (2019) Quantifying riverine recharge impacts on redox conditions and arsenic release in groundwater aquifers along the red river, Vietnam. *Water Resour. Res.* **55**, 6712–6728.

Nickson R. T., McArthur J. M., Ravenscroft P., Burgess W. G. and Ahmed K. M. (2000) Mechanism of arsenic release to groundwater, Bangladesh and West Bengal. *Appl. Geochem.* **15**, 403–413.

Park J., Sanford R. A. and Bethke C. M. (2006) Geochemical and microbiological zonation of the Middendorf aquifer, South Carolina. *Chem. Geol.* **230**, 88–104.

Polizzotto M. L., Harvey C. F., Li G., Badruzzman B., Ali A., Newville M., Sutton S. and Fendorf S. (2006) Solid-phases and desorption processes of arsenic within Bangladesh sediments. *Chem. Geol.* **228**, 97–111.

Polizzotto M. L., Kocar B. D., Benner S. G., Sampson M. and Fendorf S. (2008) Near-surface wetland sediments as a source of arsenic release to ground water in Asia. *Nature* **454**, 505–508.

Polizzotto M. L., Lineberger E. M., Matteson A. R., Neumann R. B., Badruzzaman A. B. M. and Ashraf Ali M. (2013) Arsenic transport in irrigation water across rice-field soils in Bangladesh. *Environ. Pollut.* **179**, 210–217.

Postma D., Larsen F., Minh Hue N. T., Duc M. T., Viet P. H., Nhan P. Q. and Jessen S. (2007) Arsenic in groundwater of the Red River floodplain, Vietnam: Controlling geochemical processes and reactive transport modeling. *Geochim. Cosmochim. Acta* **71**, 5054–5071.

Postma D., Jessen S., Hue N. T. M., Duc M. T., Koch C. B., Viet P. H., Nhan P. Q. and Larsen F. (2010) Mobilization of arsenic and iron from Red River floodplain sediments, Vietnam. *Geochim. Cosmochim. Acta* **74**, 3367–3381.

Postma D., Larsen F., Thai N. T., Trang P. T. K., Jakobsen R., Nhan P. Q., Long T. V., Viet P. H. and Murray A. S. (2012) Groundwater arsenic concentrations in Vietnam controlled by sediment age. *Nat. Geosci.* **5**, 656–661.

Rahman M. A., Rahman M. M., Ahmed A. T. A., Mollah A. R., Hossain M. A., Resources M. and Discipline T. (2008) A survey on the diversity of freshwater crabs in some wetland ecosystems of bangladesh. *Int. J. Sustain. Crop Prod.* **3**, 10–17.

Roberts L. C., Hug S. J., Dittmar J., Voegelin A., Saha G. C., Ali M. A., Badruzzaman A. B. M. and Kretzschmar R. (2007) Spatial distribution and temporal variability of arsenic in irrigated rice fields in Bangladesh. 1. Irrigation Water. *Environ. Sci. Technol.* **41**, 5960–5966.

Roberts L. C., Hug S. J., Voegelin A., Dittmar J., Kretzschmar R., Wehrli B., Saha G. C., Badruzzaman A. B. M. and Ali M. A. (2011) Arsenic dynamics in porewater of an intermittently irrigated paddy field in Bangladesh. *Environ. Sci. Technol.* **45**, 971–976.

Schroth A. W., Bostick B. C., Graham M., Kaste J. M., Mitchell M. J. and Friedland A. J. (2007) Sulfur species behavior in soil organic matter during decomposition. *J. Geophys. Res. Biogeosciences* **112**, 1–10.

Seddique A. A., Masuda H., Mitamura M., Shinoda K., Yamanaka T., Itai T., Maruoka T., Uesugi K., Ahmed K. M. and Biswas D. K. (2008) Arsenic release from biotite into a Holocene groundwater aquifer in Bangladesh. *Appl. Geochemistry* **23**, 2236–2248.

Seddique A. A., Masuda H., Mitamura M., Shinoda K., Yamanaka T., Nakaya S. and Ahmed K. M. (2011) Mineralogy and geochemistry of shallow sediments of Sonargaon, Bangladesh and implications for arsenic dynamics: Focusing on the role of organic matter. *Appl. Geochem.* **26**, 587–599.

Sengupta S., McArthur J. M., Sarkar A., Leng M. J., Ravenscroft P., Howarth R. J. and Banerjee D. M. (2008) Do ponds cause arsenic-pollution of groundwater in the Bengal basin? An answer from West Bengal. *Environ. Sci. Technol.* **42**, 5156–5164.

Smith A. H., Lingas E. O. and Rahman M. (2000) Contamination of drinking-water by arsenic in Bangladesh: a public health emergency. *Bull. World Health Organ.* **78**, 1093–1103.

Stahl M. O., Tarek M. H., Yeo D. C. J., Badruzzaman A. B. M. and Harvey C. F. (2014) Crab burrows as conduits for groundwater-surface water exchange in Bangladesh. *Geophys. Res. Lett.* **41**, 8342–8347.

Stahl M. O., Harvey C. F., van Geen A., Sun J., Thi Kim Trang P., Mai Lan V., Mai Phuong T., Hung Viet P. and Bostick B. C. (2016) River bank geomorphology controls groundwater

arsenic concentrations in aquifers adjacent to the Red River, Hanoi Vietnam. *Water Resour. Res.* **52**, 6321–6334.

Stuckey J. W., Schaefer M. V., Kocar B. D., Benner S. G. and Fendorf S. (2016) Arsenic release metabolically limited to permanently water-saturated soil in Mekong Delta. *Nat. Geosci.* **9**, 70–76.

Swartz C. H., Blute N. K., Badruzzman B., Ali A., Brabander D., Jay J., Besancon J., Islam S., Hemond H. F. and Harvey C. F. (2004) Mobility of arsenic in a Bangladesh aquifer: Inferences from geochemical profiles, leaching data, and mineralogical characterization. *Geochim. Cosmochim. Acta* **68**, 4539–4557.

Uddin M. N. and Abdullah S. K. M. (2003) Quaternary geology and aquifer systems in the Ganges-Brahmaputra-Meghna delta complex, Bangladesh. In *Proc. GEOSAS-IV, Geol. Surv. India*, pp. 400–416.

Wagle P. V. (1924) Land Crabs as Agricultural Pests in Western India. *Dept. Agric. Bombay Bull.*, 118.

Weinman B., Goodbred S. L., Zheng Y., Aziz Z., Steckler M., van Geen A., Singhvi A. K. and Nagar Y. C. (2008) Contributions of floodplain stratigraphy and evolution to the spatial patterns of groundwater arsenic in Araihazar, Bangladesh. *Geol. Soc. Am. Bull.* **120**, 1567–1580.

Wu T., Shelobolina E., Xu H., Konishi H., Kukkadapu R. and Roden E. E. (2012) Isolation and microbial reduction of Fe(III) phyllosilicates from subsurface sediments. *Environ. Sci. Technol.* **46**, 11618–11626.

Yu W. H., Harvey C. M. and Harvey C. F. (2003) Arsenic in groundwater in Bangladesh: A geostatistical and epidemiological framework for evaluating health effects and potential remedies. *Water Resour. Res.* **39**, 1–17.

Associate editor: Karen Johannesson